AD-A129 640 O DBI ANTENNA(U) HAZELTINE CORP GREENLAWN NY 1/1
E M NEWMAN ET AL. DEC 81 6455 DAAK80-79-C-0279

UNCLASSIFIED F/G 9/5 NL

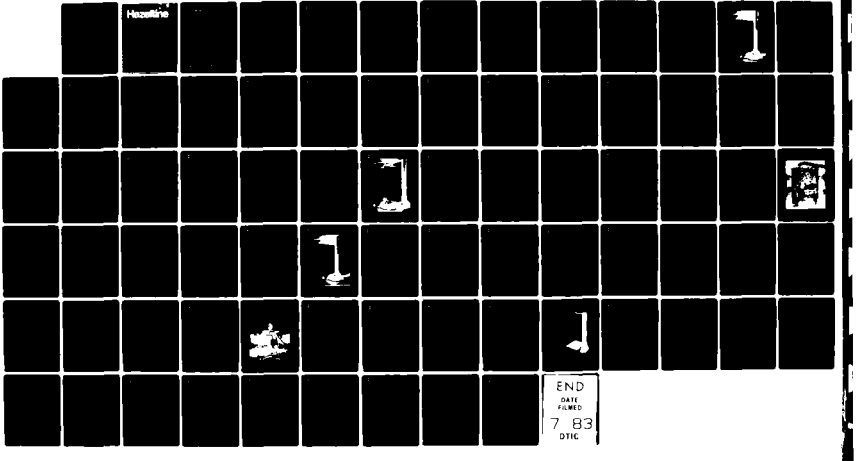

END
DATE FILMED
7 83
DTIC

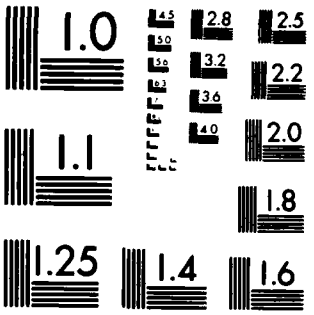

Hazeltine
Corporation
Greenlawn, N.Y. 11740 (516) 261-7000

(11)

Report 6455
FINAL TECHNICAL REPORT
0 dBi ANTENNA

Contract DAAK-80-79-C-0279

Contract No. DAAK80-79-C-0279

December 1981

Prepared by: E. M. Newman
E. M. Newman
Program Manager

C. M. Ruskowski
C. M. Ruskowski
Antenna Engineer

Approved by: A. J. Kelly /emn
A. J. Kelly
Wheeler Laboratory Head

ACTIVE SHEET RECORD

Total number of pages in this publication is 78 consisting of the following:

Page	Rev #	Added Pages	
		Page	Rev #
Title	Orig		
ASR-1			
i			
iv			
1-1			
1-6			
2-1			
2-18			
3-1			
3-20			
4-1			
4-24			
5-1			
5-2			
6-1			
6-2	Orig		

Page	Rev #	Added Pages	
		Page	Rev #

C80038

CONTENTS

ILLUSTRATIONS

ILLUSTRATIONS

TABLES

ABBREVIATIONS AND ACRONYMS

The abbreviations and acronyms used in this document are listed below. This list does not include abbreviations and acronyms that are in accordance with MIL-STD-12.

AVRADA	Aviation Research and Development Agency
NOE	Nap of the Earth
RTV	Room Temperatuire Vulcanizing
SINCGARS	Single Channel Ground and Air Radio System

SECTION I

INTRODUCTION

1.1 GENERAL

This report describes the design, development, and test of a high efficiency antenna for use on rotary wing and fixed wing Army aircraft. The antenna is intended to provide efficient performance for Army VHF/FM and Single Channel Ground and Air Radios (SINCGARS) located on helicopters. The objective of this effort, performed by Hazeltine Corporation under contract DAAK80-79-C-0279, was to demonstrate the feasibility of a SINCGARS compatible antenna which would allow Army aircraft to communicate more effectively, especially in Nap of the Earth (NOE) operation. This report covers the work performed during the period beginning August 31, 1979 and ending August 31, 1981.

1.2 DESIGN OBJECTIVES

The configuration and design of this antenna were dictated largely by three different requirements. First, the antenna had to be compatible with existing and future rotary wing aircraft, meaning that small size, light weight, low drag, and low power consumption were required. Second, the antenna had to be compatible with future NOE radio systems. This meant that the antenna had to have voltage standing wave ratio (VSWR) characteristics compatible with anticipated solid-state power amplifiers, and a radiation efficiency that was substantially higher than any existing helicopter antenna. Finally, the antenna had to be compatible with anticipated requirements for the future SINCGARS. Because the SINCGARS system is a frequency hopping system, the antenna had to be either broadband or have tuning with speed compatible with a fast frequency hop system. The design objective of 100-microsecond switching time is compatible with the fastest anticipated SINCGARS frequency hopping rate.

The design requirements as specified in Aviation Research and Development Agency (AVRADA) statement of work, dated 8 April 1979, are listed below:

- o Gain: 0 dBi
- o Directivity: Omnidirectional azimuthal pattern
- o Frequency Range: 30 to 88 MHz
- o VSWR: 2 to 1 maximum
- o Power Capacity: 60 watts average and 110 watts peak

- o Size/Form Factor: Design consistent with application for rotary wing aircraft
- o Tuning: Fully automatic, tune on receive or transmit, 100-microsecond tuning time, compatible with ARC-114

1.3 ALTERNATIVE ANTENNA DESIGNS

Several alternative antenna design approaches can be considered for achieving the design objectives listed above. These alternatives can be separated into two categories, each with several subcategories. First, the antenna can be designed as a broadband element requiring no tuning information, or a tunable element requiring tuning information from the associated radio. Both of these approaches are in use in some form in the existing Army inventory of antennas for VHF/FM.

Broadband antennas have the advantage of requiring no complex tuning interface. They, therefore, tend to be simple and low cost. However, this simplicity is achieved at the expense of low efficiency, since the broadband element must give up efficiency to achieve the wideband impedance matching that is required. Based on other Hazeltine design work, we estimate that a broadband antenna of this type would have an efficiency relative to a monopole of -6 to -10 dB. Measurements made by Army personnel on the existing FM10-30 antenna show a gain at 30 MHz, compared to a reference dipole, of -17 dB.

This loss in efficiency in a broadband antenna could be overcome by adding an integral high power amplifier as part of the antenna design. The combination of the power amplifier and antenna must be designed to provide the required effective radiated power. While this approach is possible, it poses significant practical difficulties. For example, we estimate that a broadband antenna might operate at 17% efficiency at 30 MHz. Assuming that 42 watts are required to be radiated, the amplifier must be designed to deliver 252 watts to a 50-ohm load. Assuming class C operation with an efficiency of 75%, the input power must be 336 watts, with 294 watts dissipated in the amplifier under worst case conditions. Obviously, the problems associated with dissipating 294 watts are significant, and the power required to operate the antenna/amplifier system is substantial.

The alternative is a tunable antenna. Although more complex than a broadband antenna, the tunable antenna has the advantage of inherently high efficiency for a given size.

The tunable antenna is more efficient because the performance is achieved over a relatively narrow frequency band which is consistent with the capabilities of the small antenna element. (The trade-off of antenna size and bandwidth capability is discussed further in Section 2.) A variety of options in a tunable antenna design are available. For example, the antenna may be continuously tuned using analog techniques, or may be tuned in operating bands using switching circuits. Also, the tuning may be done using electronic devices such as positive intrinsic negative (PIN) diodes, or electromechanical devices such as variable capacitors and inductors. Further, the tuning may be done on an open loop or closed loop basis. An open loop system is one in which tuning information is made available to the antenna, which then relies only on the tuning information to select the appropriate tuning element settings. A closed loop system is one in which the antenna senses a particular parameter, usually reflected voltage amplitude and phase, and automatically adjusts the tuning element to achieve the desired value of the parameter (usually minimum reflected voltage).

Each of the design approaches described above has relative advantages and disadvantages. For example, the closed loop system relies upon transmitter power to perform its tuning function. This results in undesired and non-useful radio transmissions to allow the antenna to tune to the operating frequency. Open loop systems, on the other hand, require a specific interface with the radio transmitter on board the aircraft. However, the statement of work has defined the tuning approach because of two requirements: first, the antenna is not allowed to use transmitter power to perform a tuning function; and second, the tuning time must be accomplished in less than 100 microseconds. Because of these requirements, a tunable antenna is constrained to be an open loop electronically tuned type of system.

The alternatives described above were considered by Hazeltine during the initial design efforts. We concluded that an open loop electronically tuned antenna was the most practical approach in meeting the design requirements. The key features of the antenna design are described below in subsection 1.4.

1.4 ZERO DBI ANTENNA

Figure 1-1 shows a photograph of the Hazeltine zero dBi antenna. The radiating element consists of the vertical stalk and the two top horizontal radials. The radials

Figure 1-1. Hazeltine's Zero dBi Antenna

increase the electrical length of the antenna. The bulge at the bottom of the antenna contains the diode switching and tuning circuits. The small box located next to the antenna contains the digital logic and driver circuits used to convert the frequency information from the ARC-114 into appropriate diode biases.

Figure 1-2 shows the antenna block diagram. The antenna is tuned in six bands which provide coverage from 30 to 88 MHz. Each band has a separate set of components for matching the band. The bands are selected using the diodes shown in figure 1-2. The diodes essentially form two single-pole six-throw switches, which connect the appropriate matching network.

The logic consists of two comparator chips, which are used to decode the analog frequency information from the ARC-114, a programmable logic array (PLA) chip, which is programmed to determine which band is connected at a given frequency, and a set of drivers which actually bias the diodes. The interface unit also contains both low and high voltage power supplies for the diode bias.

Key antenna design tradeoffs are discussed in Section 2, and a detailed description of the antenna is contained in Section 3. Section 4 presents the results of testing the antenna.

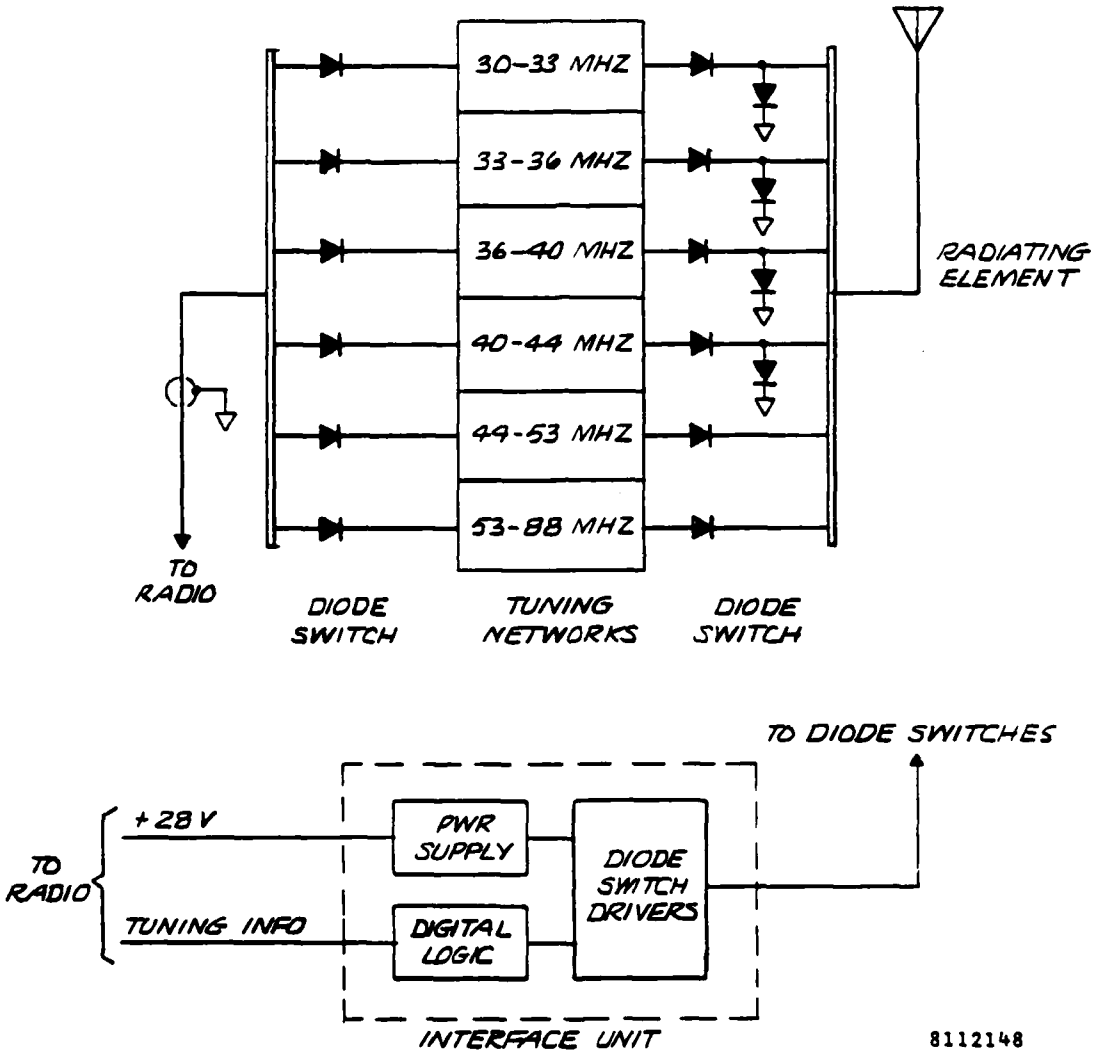

Figure 1-2. Zero dBi Antenna Block Diagram

SECTION II

ANTENNA DESIGN TRADEOFFS

2.1 ELEMENT LOCATION

The location of the antenna element influences the radiation patterns at the frequencies of operation. During the initial study phase of the program, alternative antenna locations on the OH-58A were investigated.

Locations were considered which permitted the physical mounting of the antenna, provided reasonably omnidirectional azimuth patterns, and produced the maximum of the elevation pattern near the horizon.

Figure 2-1 shows some alternative locations for a VHF-FM antenna on the OH-58A. Most of these locations have been analyzed by McDonnell Douglas Research Laboratories (Section 6, ref 1). Their results, one example of which is shown in figure 2-2, are useful for comparing antenna locations. Their neglect of rotor effects, however, means that their data could be in error by several dB.

The impedance of the antenna element also is affected by the location on the airframe. The helicopter is small enough in wavelengths so that it does not appear as an infinite flat ground plane. At 30 MHz, the OH-58A is approximately one wavelength long. An antenna mounted at the end of the tail boom will see an even smaller ground plane.

Two antenna locations were of special interest. The first was location "A" shown in figure 2-1 - the present location for the bent whip VHF-FM antenna. As shown in figure 2-3, the antenna exhibits good omnidirectional characteristics (4 dB), and almost uniform elevation coverage from -15 to +15^{o} relative to the horizon. Measured azimuth patterns agree qualitatively with the calculated patterns.

This location has a relatively large, flat area to act as a ground plane. It also allows short, low loss, cable runs from the transmitter to the antenna. On the other hand, the proximity of the canopy windows and rotor blade may affect the patterns of the antenna.

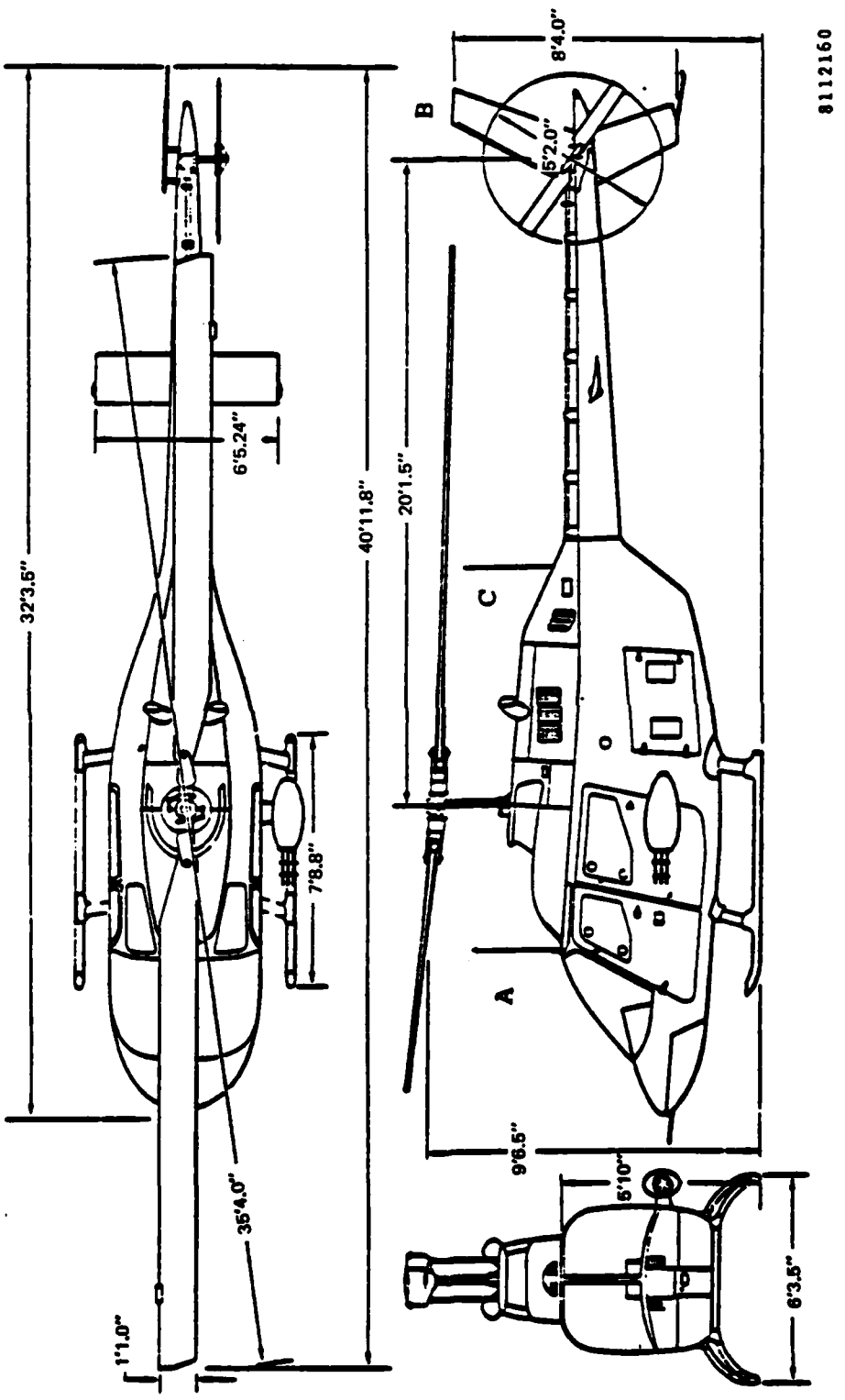

Figure 2-1. Alternative Antenna Locations on OH-58A

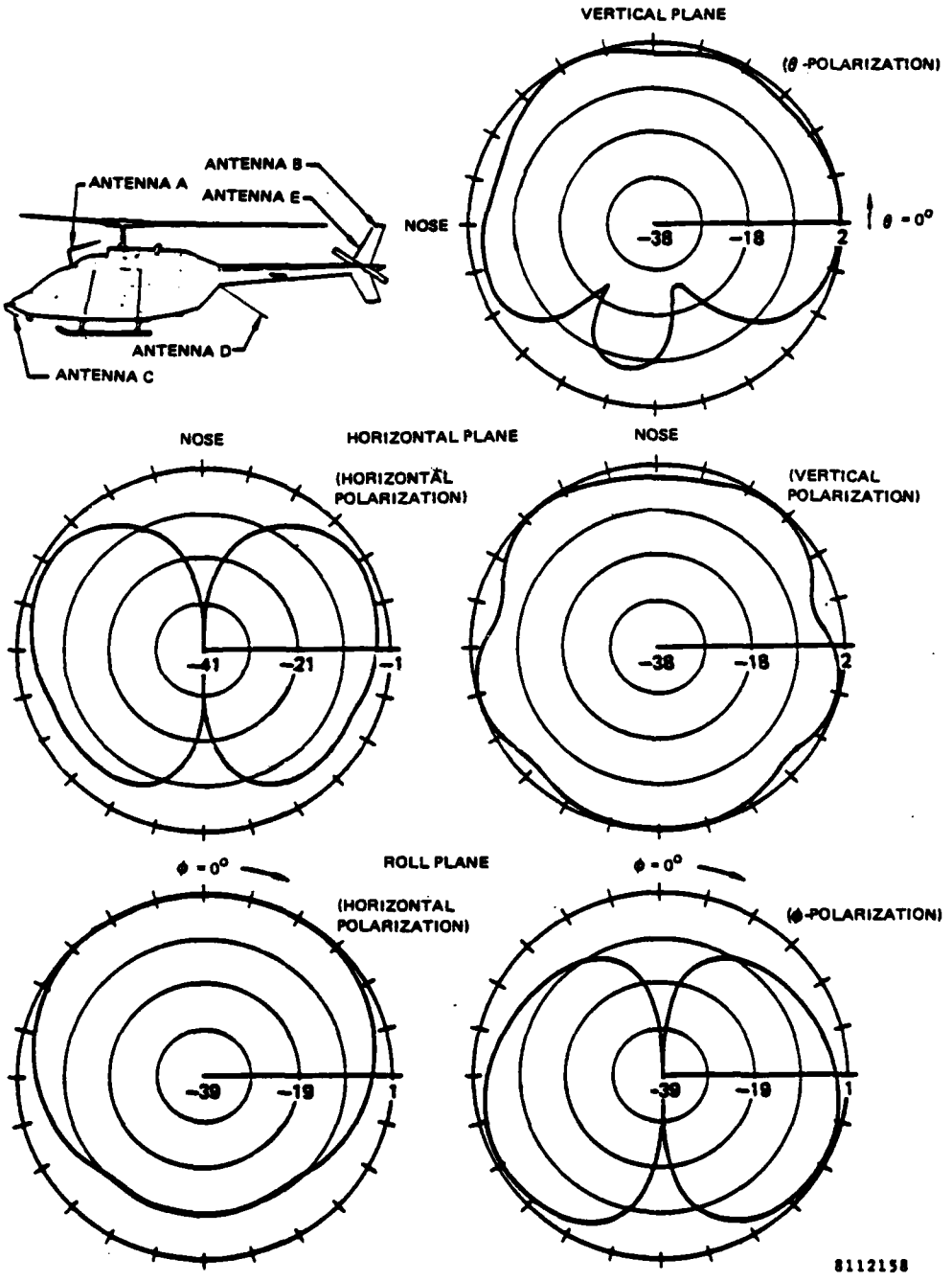

Figure 2-2. Computed Power Gain Patterns in Free Space for OH-58A at 61.65 MHz, Antenna Type A (from ref 1)

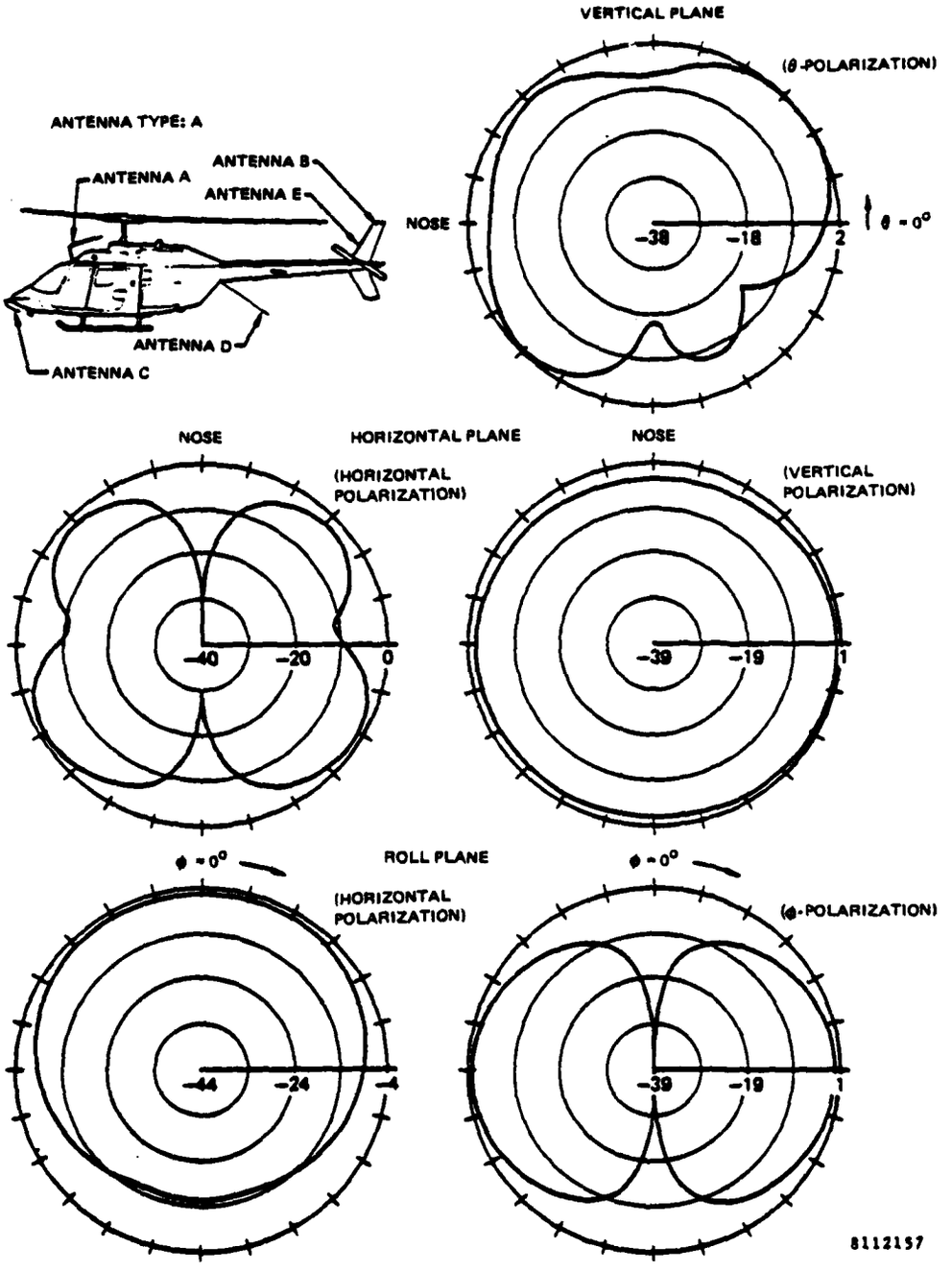

Figure 2-3. Computed Power Gain Patterns in Free Space for OH-58A at 30 MHz (from ref 1)

A second location which was considered is shown as "C" in figure 2-1. Calculated patterns are not available for this location. However, based on the patterns of configuration D (ref 1) as shown in figure 2-4, the antenna should have good omnality. The location at the center of the aircraft provides a good ground plane for the radiator. Also, the cable run to the antenna is approximately half that of the tailfin-mounted antenna.

Inspection of the OH-58A helicopter revealed that location "C" was not suitable for antenna mounting. The drive shaft for the tail rotor passes through the location, and the cover must be removable for servicing. Thus location "A" was selected for mounting the zero dBi antenna.

The selected location offered the advantage of existing mounting holes, existing cable runs, and relatively good pattern coverage.

2.2 ELEMENT CONFIGURATION

The element configuration was selected to optimize the fundamental tradeoffs between size, bandwidth, and efficiency. A radiating element with maximum bandwidth for its height was selected.

The radiating element for the VHF-FM antenna was restricted in height by several factors: clearance of the rotors, aerodynamic drag, and structural strength. All three factors make a low antenna advantageous, although the first factor is clearly the most compelling. A height of 30 inches as a maximum was initially selected, based on the rotor clearance of approximately 40 inches, to approximate the overall height of the bent whip (FM -10-30-1) which is about 27 inches.

Subsequent discussions with maintenance personnel at Lakehurst revealed that, during flight, the rotors of the OH-58 may approach within 30 inches of the cabin roof. Based on this information, the height of the antenna was reduced from 30 to 27 inches. The final matching network design was based on the lower 27-inch height. This is a significant change, since for a small antenna the power factor is related to the cube of antenna height.

For an electrically small monopole (such as our 27-inch antenna at 30 MHz), the impedance bandwidth is proportional to the power factor. The power factor of the antenna at a given frequency is approximately the radiation resistance divided by the reactance. Thus, to maximize the element

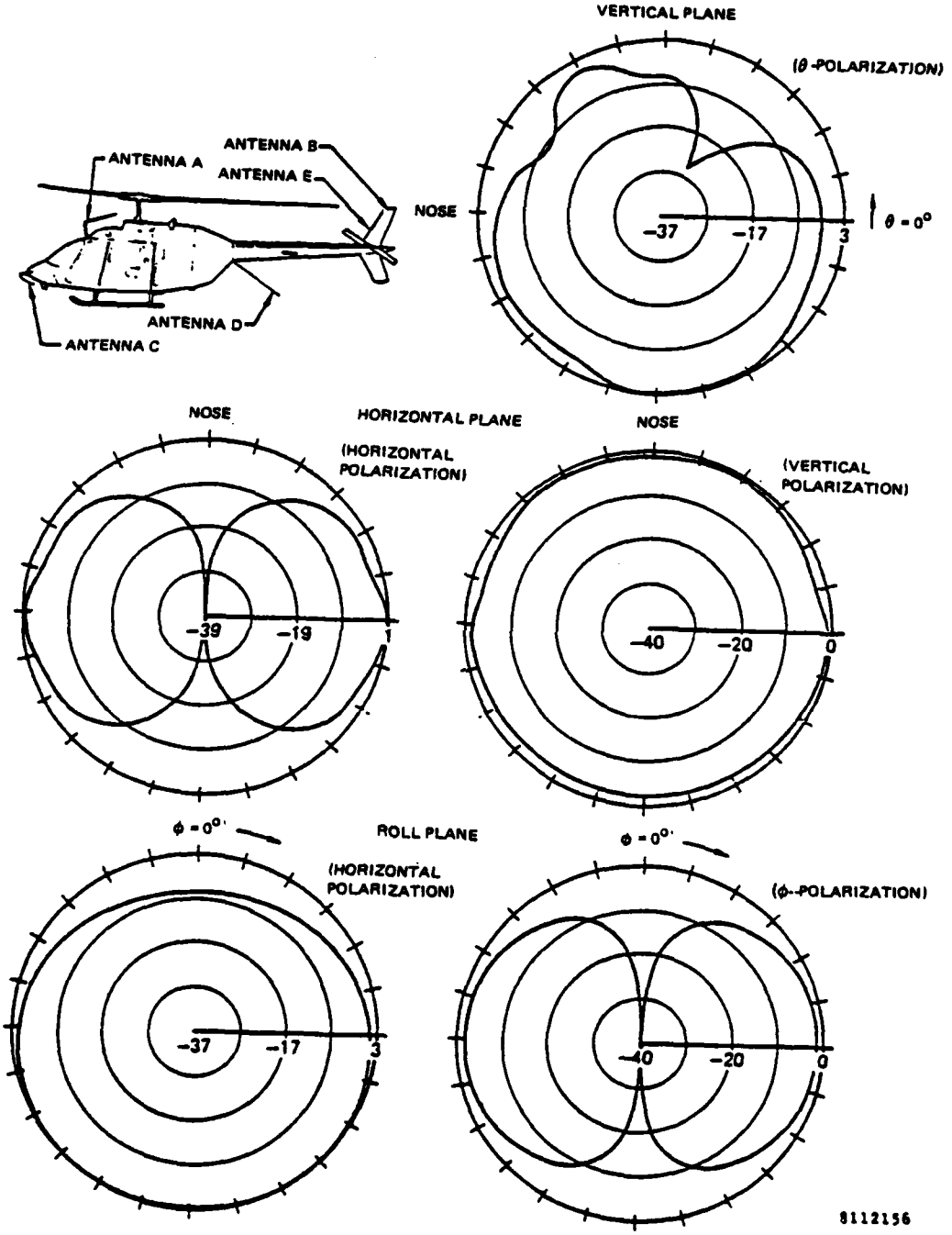

Figure 2-4. Computed Power Gain Patterns in Free Space for OH-58A at 6145 MHz, Antenna Type D (from ref 1)

bandwidth, the ratio of resistance to reactance should be maximized. Figure 2-5 shows some simple formulas derived by H. A. Wheeler (ref 2) for resistance and reactance of monopole elements. As expected, the fatter blade element has a wider bandwidth (greater power factor) than a thin monopole of the same height. A higher element, of course, also has a wider bandwidth. The equation shows that a 30-inch by 15-inch blade can have the same bandwidth as a 52-inch whip.

The final element configuration is shown in figure 2-6; the power factor has been maximized by a combination of a wide element (5 inches) and top loading wires.

2.3 MATCHING NETWORK DESIGN

The function of the antenna tuning network is to transform the radiating element impedance to a nominal resistance (usually 50 ohms) over a specified frequency band and for a given VSWR tolerance. Fundamental limitations have been defined for the match and bandwidth achievable by tuning networks. For example, R. M. Fano has calculated curves for a small antenna which can be represented by a series resonant circuit (ref 3). Figure 2-7(a) shows how the reflection of the antenna is a function of the antenna bandwidth, the operating bandwidth, the required VSWR, and the complexity of the tuning network.

As an example, consider the selected top-loaded blade. As presented in subsection 2.2, the element itself has a power factor (ratio of radiation resistance to reactance) of 0.065 at 30 MHz. First, suppose the element is single tuned, meaning that one circuit element is added, as shown in figure 2-7(b). The curves show that the element can be matched to a 2 to 1 VSWR over a bandwidth equal to approximately 0.5 x PF; therefore, the operating bandwidth will be 0.5 x 0.065 x 30 or 0.98 MHz. If a double-tuned matching circuit is used (as shown in figure 2-7), the bandwidth increases from 0.5 to about 1.6, corresponding to 3.1 MHz. If an infinite number of circuits were added, the bandwidth would increase to approximately 5.6 MHz.

While these curves are useful in estimating antenna bandwidth, they must be used with care. The derivation assumes an antenna element that can be represented by a simple series resonant circuit with a resistance in series. The small element does not have a constant resistance and, at the high end of the 30 to 88 MHz band, the element is not a simple resonant circuit. Thus, the curves can provide very

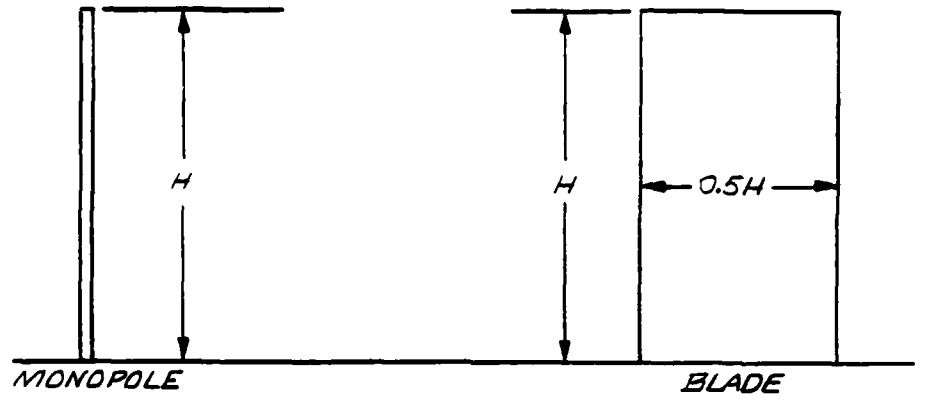

Figure 2-5. Resistance and Reactance of Monopole Elements

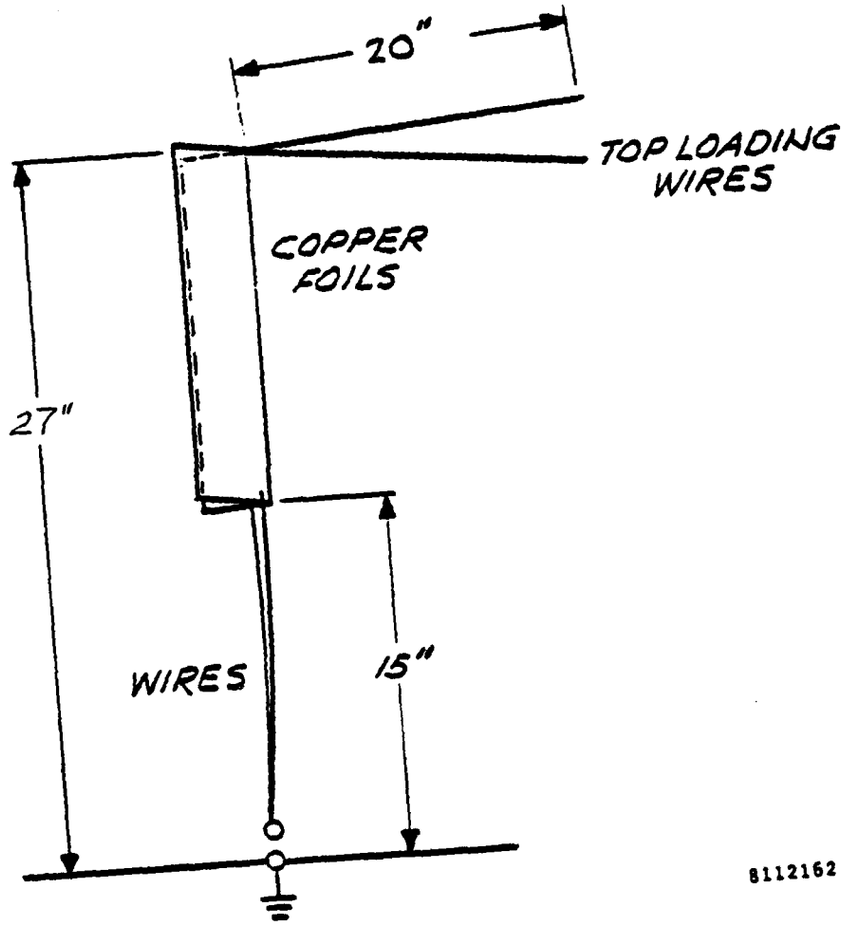

Figure 2-6. Final Radiator Configuration for Zero dBi Antenna

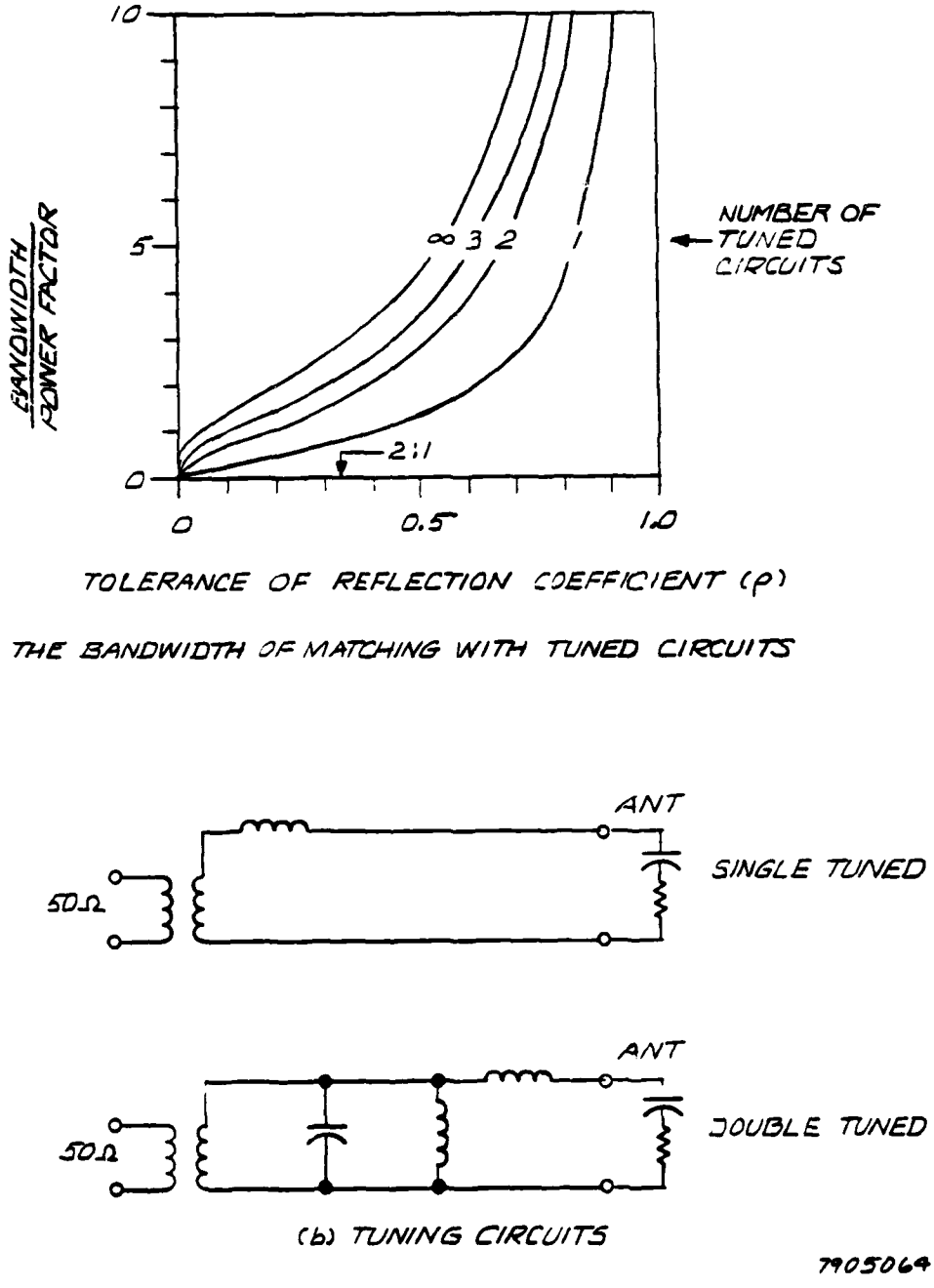

Figure 2-7. Limitation of Antenna Tuning Networks

accurate information only for relatively narrow bandwidths. The curves provide accurate information for the 27-inch blade at 30 to 50 MHz.

The bandwidth of the individual tuning bands also is influenced by other antenna components. For example, shunt capacitance across the antenna feedpoint will reduce the bandwidth. During the design effort, the diode reverse bias capacitance and the capacitance of the diode heat sinks were evaluated. The final number of bands selected was six. This was based on actual measurements of the antenna impedance on the OH-58A.

The matching circuit for each band was carefully adjusted to achieve the lowest VSWR over the entire band. All of the bands used double-tuned circuits; this represented the best compromise between bandwidth and circuit complexity. The resulting matching network is described in detail in Section 3.

The matching network components were selected to provide the lowest possible loss consistent with the packaging requirements. All inductors were air wound of heavy wire, and all capacitors were selected to have a Q greater than 500. The low loss components benefited the antenna in two ways: the gain of the antenna was not reduced significantly, and the 60-watt power capacity of the antenna was achieved.

The inductors were designed to be shielded so that they could be closely spaced without coupling. Formulas for inductance and inductor Q were provided by Dr. Wheeler (ref 3). These formulas were used to design the required inductors. Figure 2-8 shows the results of initial evaluations of some sample inductors.

The measured values of shielded inductance were about 5% higher than those attained theoretically. The theoretical values were attained using an inductance chart and the physical dimensions of the measured coil. The measured Q was about 50% lower than calculated, but was still acceptable.

2.4 DIODE SWITCHING

Diode switching of the matching networks is the key to achieving the design goal of 100-microsecond switching time. Considerable attention was given to selecting diodes and their associated circuits.

	Q MEASURED	L uH MEASURED	Q MAX THEORETICAL	L uH THEORETICAL	% Q VARIATION	% L VARIATION
UNSHIELDED	240	0.450	480	0.40	50%	11%
SHIELDED SHUNT	240	0.428	480	0.40	50%	6%
SHIELDED SERIES	240	0.423	480	0.40	50%	5%

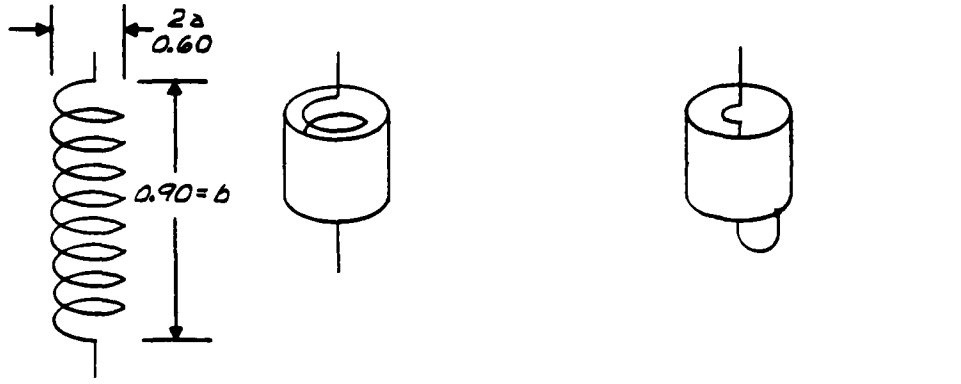

Figure 2-8. Design of High-Q Inductors for Zero dBi Antenna

Figure 2-9 shows in block diagram form the diode switching in the antenna. The input and output series diodes are used to switch the matching networks in and out. The shunt diodes on the output side are used to achieve high isolation between the bands.

Special diodes were selected to minimize loss. The diodes are high voltage PIN types, noted for their ability to rapidly switch, yet also handle high RF power. Hazeltine has built a number of high power L-band switches using these types of diodes. Another attraction of the PIN diodes are the relatively low bias required. The diode can carry more RF voltage than the bias voltage without conducting over any part of the RF cycle. Thus, the diode can handle 1000 peak volts of RF with only 100 volts of bias. Similarly, the forward bias is approximately 150 mA, although the diode may handle several amperes of RF current.

Power dissipation in the forward and back-biased diodes greatly affects both the antenna efficiency and the thermal requirements of the diode heat sink. To maximize efficiency and minimize the size of the heat sink, the following restrictions were considered when selecting PIN-switching diodes:

- Low Series forward bias resistance, R_s: 0.3 ohms
- High Reverse Bias Resistance, R_f: 50K ohms
- Low Thermal Impedance, θ: 5°C/watt

Heat sinks were required to provide a low thermal resistance between the diodes and the environment. Calculations showed that an unacceptably large heat sink was required if it was enclosed completely within the fiberglass radome. To keep the antenna weight at a minimum, light aluminum heat sinks were connected to heat radiators located on the exterior of the blade; thus, the heat is radiated directly to the exterior environment. A thermal analysis showed that the diode temperatures remain within acceptable limits when the antenna is subject to 60 watts continuous input at 71°C.

Figure 2-10 shows the thermal paths used to calculate the temperature rise of the diodes in the input heat sink. Note that the thermal resistance is dominated by the transfer of heat from the external heat sink to the outside air. The resulting diode junction temperature, with an ambient temperature of 71°C, is 110°C, which is well below the rated maximum of 175°C. Figure 2-11 shows a similar calculation for the heat sink at the antenna. This power dissipation is greater for these diodes because of the higher RF currents

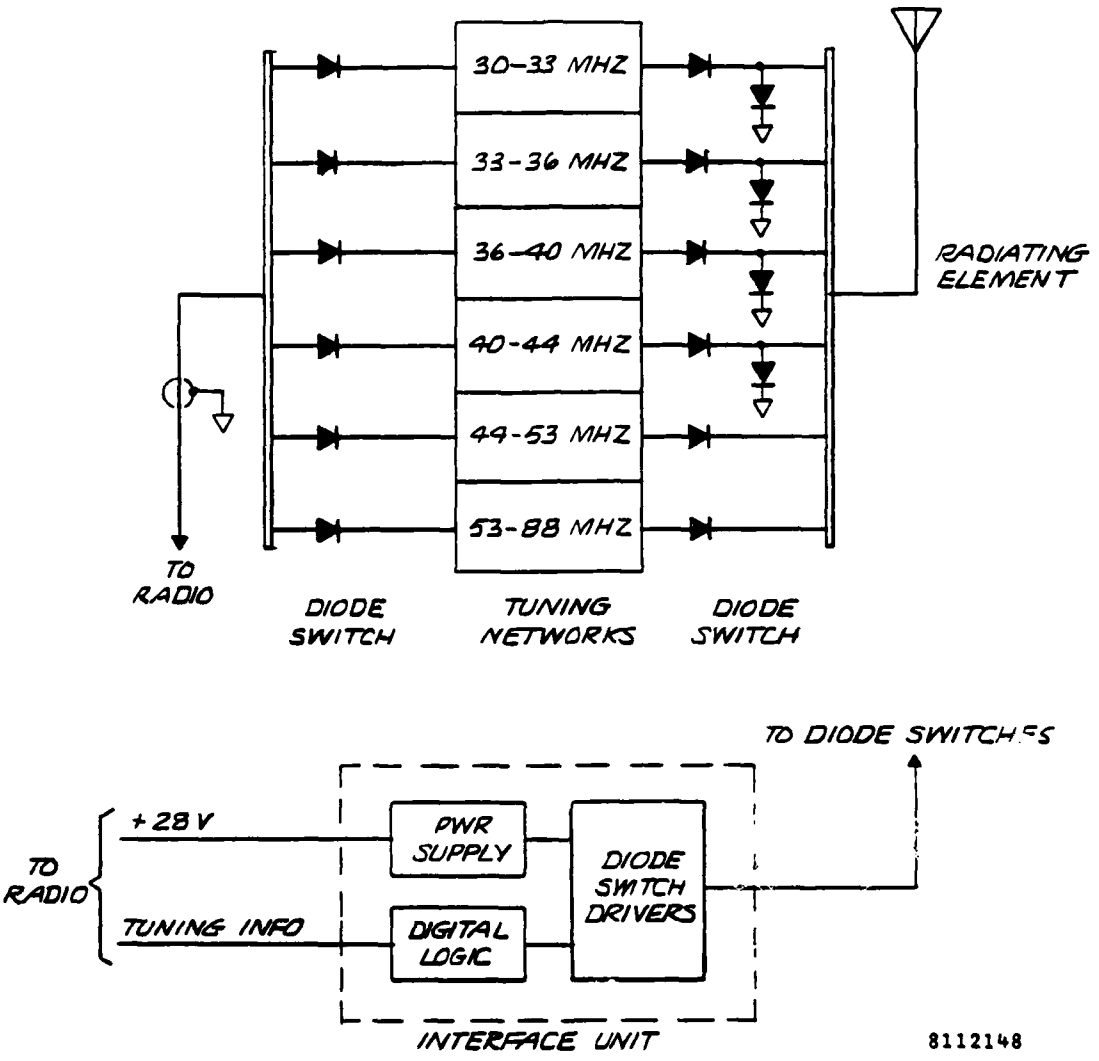

Figure 2-9. Zero dBi Antenna Block Diagram

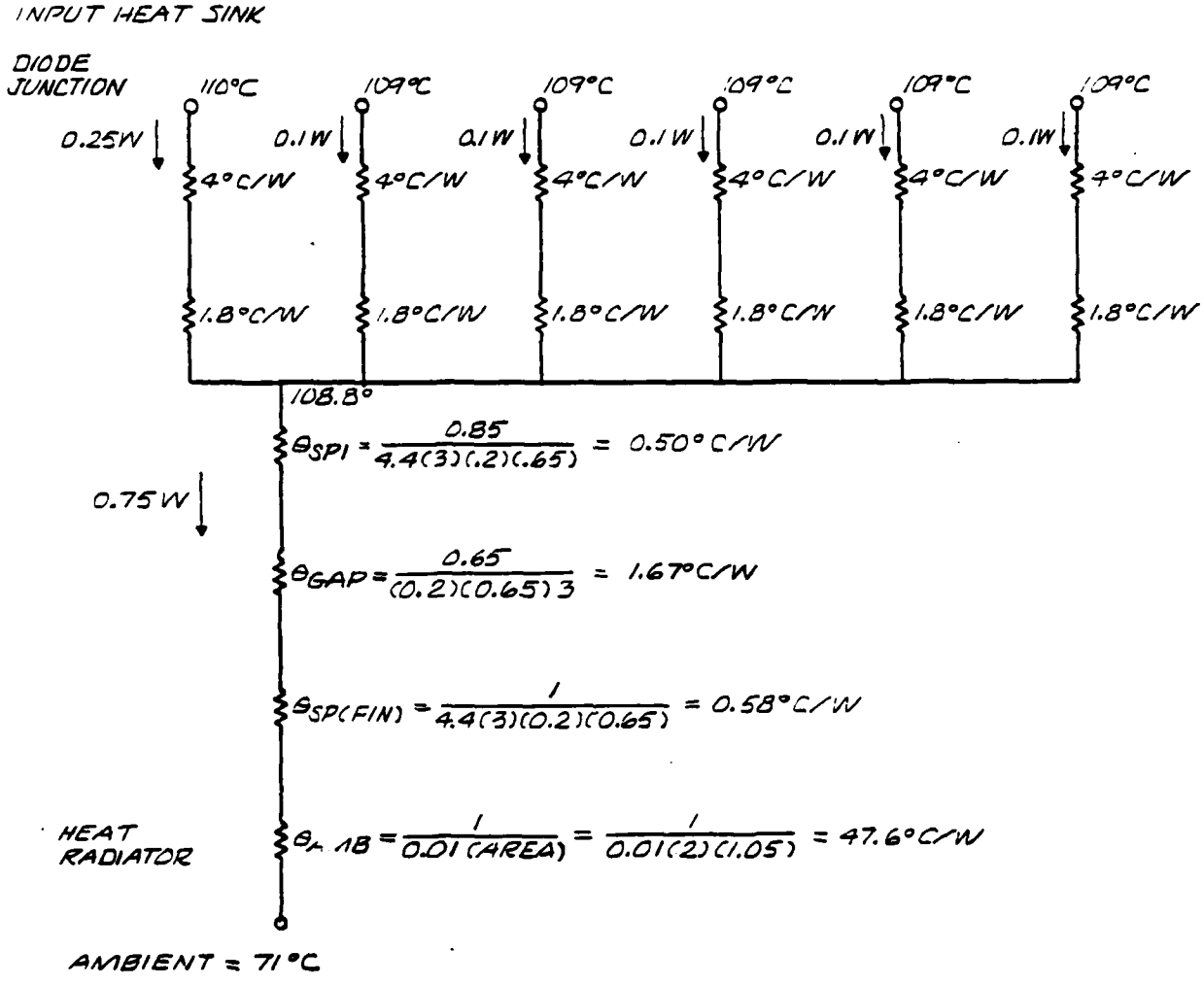

Figure 2-10. Thermal Analysis of Input Diodes

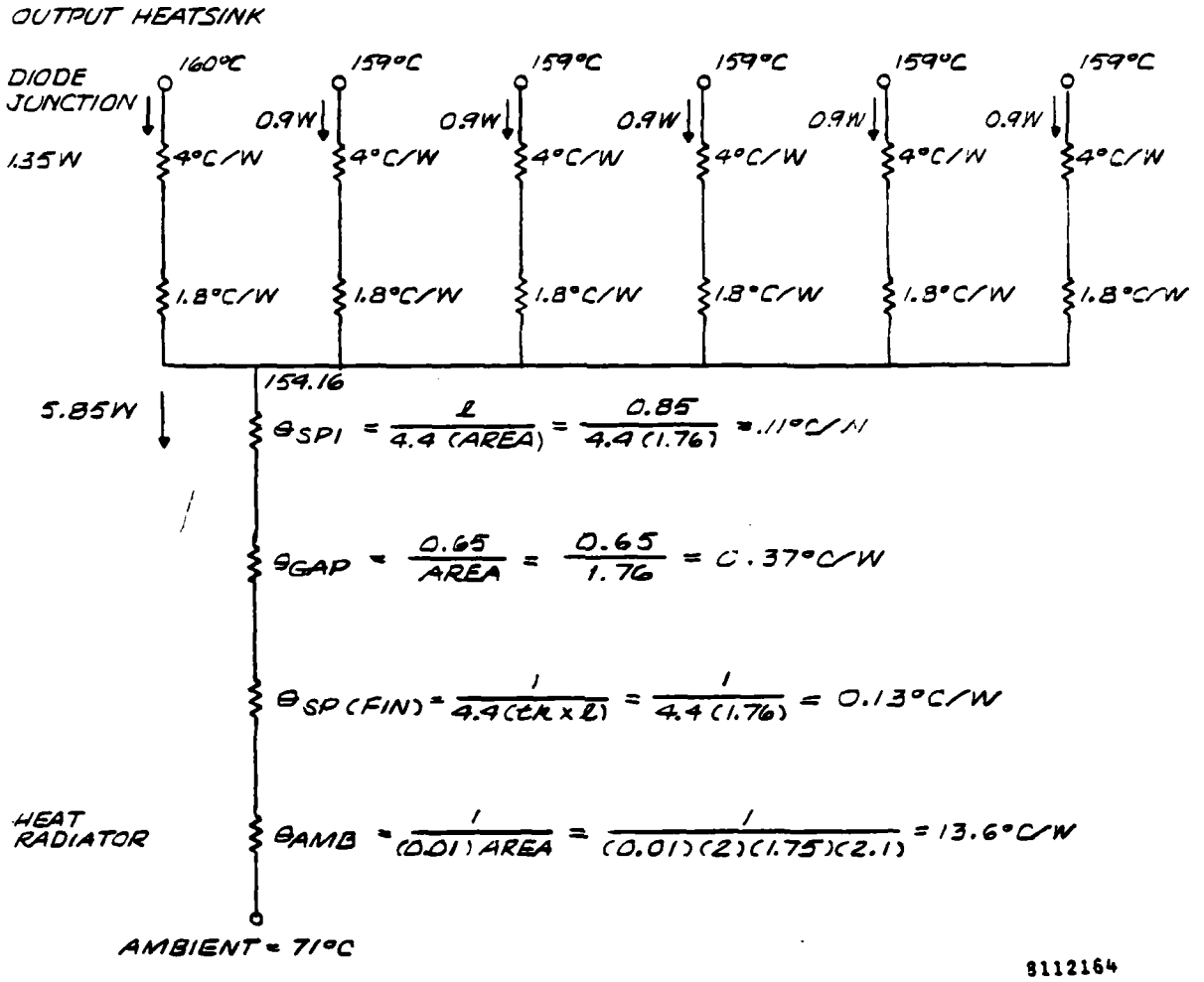

Figure 2-11. Thermal Analysis of Output Diodes

and voltages, so the resulting temperature rise is greater. Under worst case conditions, the diode junction temperature is 160°C, below the rated maximum of 175°C.

The diode and component temperature rise was the limiting factor for average power capacity.

The peak power capacity of the antenna is limited by the breakdown voltage of the diodes used in the switched tuning network. The peak input power of 110 watts corresponds to 74 volts instantaneous rms across 50 ohms. However, the diode at the output of the tuning network sees a substantially higher voltage because of the high Q of the radiating element at 30 MHz. Based on measured impedance data, the instantaneous rms voltage is 400 volts, or a peak voltage of 616 volts. The PIN diodes were selected with a 1000-volt breakdown voltage, thus affording a 2-to-1 safety factor. The peak circuit voltage of 600 volts does not represent a problem for components or layout. The dielectric strength of air is approximately 150 volts per mil, so that a spacing of 0.01 inch affords an ample safety margin. The RF voltage is significantly less at frequencies above 40 MHz because the antenna Q is less.

This page intentionally left blank

SECTION III

ANTENNA DESCRIPTION

3.1 INTRODUCTION

The final design of the antenna was based upon the design tradeoffs discussed in Section II. In addition, reliability, maintainability, environment, and product cost were considered. This section describes the final antenna design in detail and, where appropriate, discusses design modifications which may be incorporated at a later time.

Table 3-1 summarizes the objectives for the design of the Hazeltine zero dBi antenna. Most requirements are derived from the performance specified in the statement of work. Others (such as the height) were derived during the initial study phase of the program.

Figure 3-1 shows the complete antenna with its associated interface unit. The interface unit contains the digital electronics used to convert the ARC-114 radio tuning information to appropriate biases for the antenna switching diodes. The interface box can be located anywhere within the aircraft, and is connected to the antenna by a shielded multiconductor cable.

The antenna is composed of two parts: the radiating element, and the RF tuning module. The tuning module can be easily removed from the radiating element for replacement or repair.

Table 3-1. Zero dBi Antenna Design Objectives

Design Parameters	Objectives
Frequency Range	30 to 88 MHz
Number of RF Bands	Six
VSWR	2.0 to 1 maximum
Power Capacity	60 W average, 110 W peak
Pattern	Omnidirectional in azimuth
Polarization	Nominally vertical
Switching Speed	100 microseconds
Height	27 inches
Voltage Required	28 VDC
Interface	With ARC-114
Mounting	Same bolt pattern as FM 10-30-1

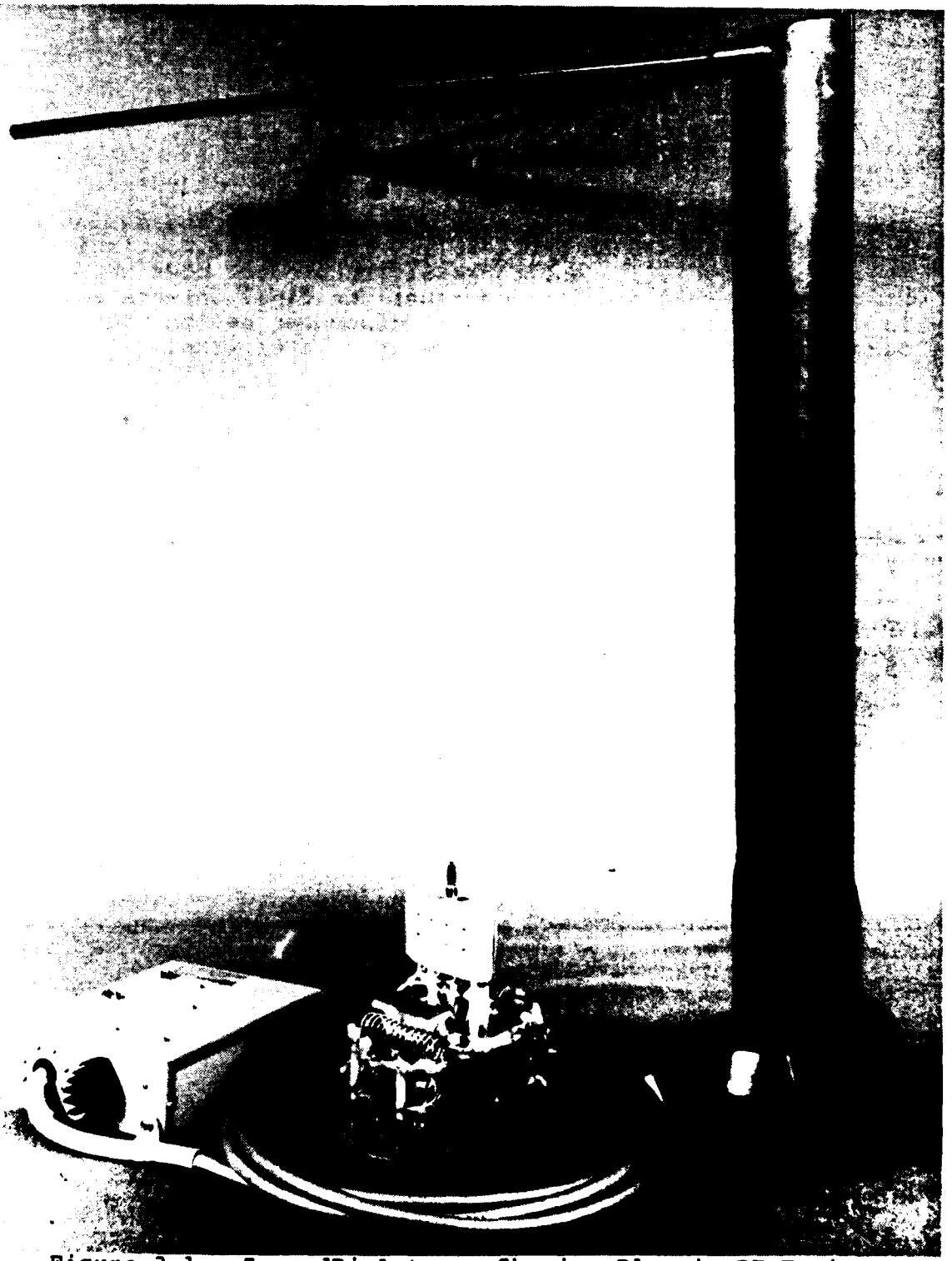

Figure 3-1. Zero dBi Antenna Showing Plug-in RF Tuning Module and Interface Unit

The following subsections describe the matching networks and diode switches, the electronic interface unit and its associated logic circuits, and the mechanical design of the antenna structure.

3.2 MATCHING NETWORK

The zero dBi antenna is matched to a 50-ohm source in six tuning bands, covering the full operating antenna bandwidth of 30 to 88 MHz. The individual RF tuning bands are:

RF Timing Band	Bandwidth, MHz
1	30 to 33
2	33 to 36
3	36 to 40
4	40 to 44
5	44 to 53
6	53 to 88

Each tuning band is switched and isolated from the other five bands through logic controlled PIN diodes. The logic voltages/currents are supplied by the interface unit, which receives power from the aircraft 28-V supply and tuning information from the ARC-114 radio.

Figure 3-2 shows the schematic of the RF tuning module. The bold vertical lines on the left and right sides of the figure represent the aluminum heat sinks for cooling the switching diodes. The left heat sink is connected to the input RF connector; the right heat sink connects to the radiating element via a plug and jack.

As can be seen in the figure, each band is switched in or out using a pair of series diodes (UM4906C). The diodes are biased in pairs, thus limiting the number of transistor drivers required.

The four low-frequency bands also contain shorting diodes. During development, it was found that the capacitance of the back biased diodes could resonate with the "off" tuning circuits to cause spurious lossy resonances in the two higher bands. To eliminate this problem, shorting diodes were added so that the resonance could not occur. The shorting diodes for a particular band are turned off when operating in that band; otherwise they are turned on.

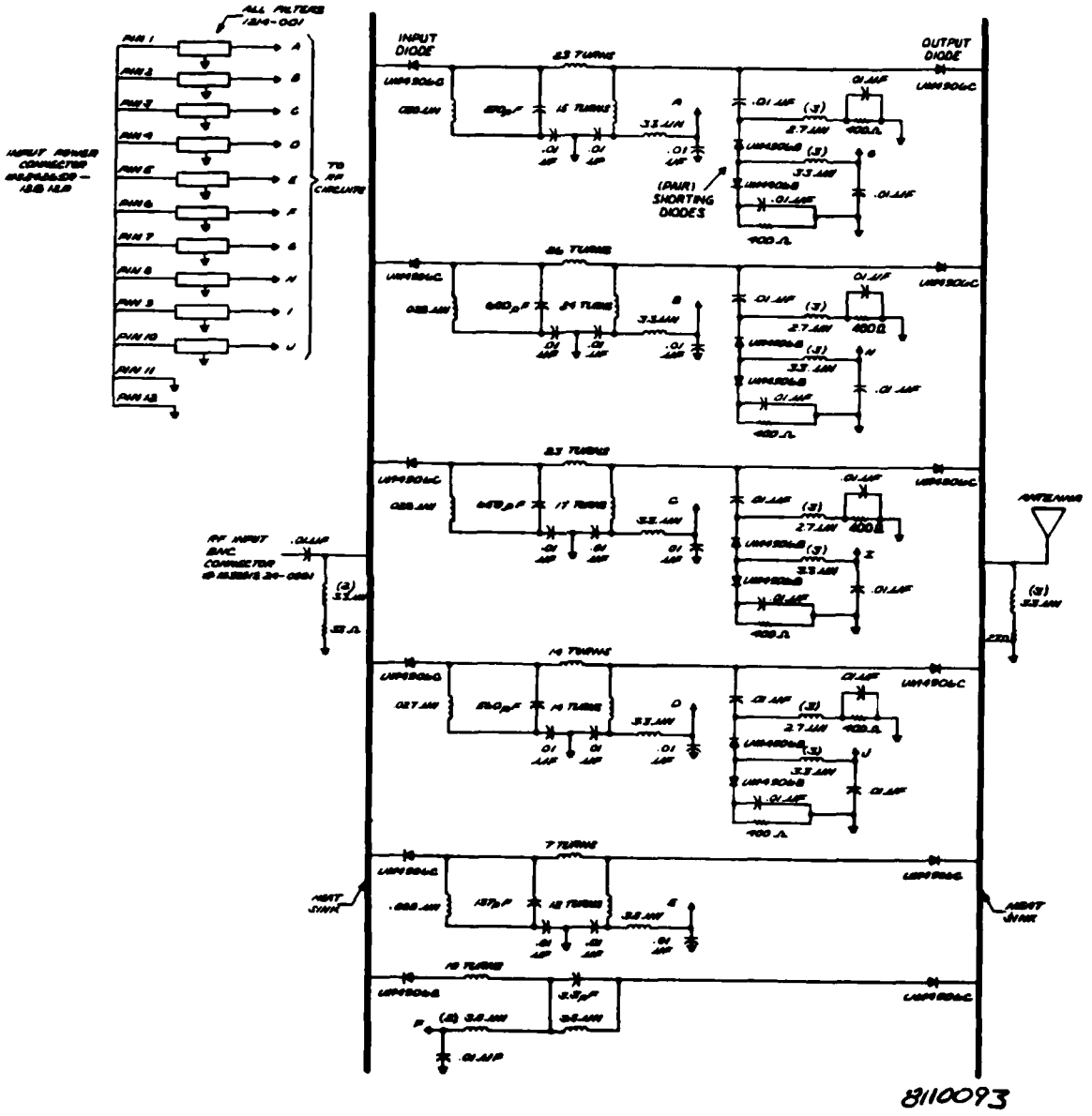

Figure 3-2. RF Tuning Module Schematic

The diodes are biased at +4 V (on) and -100 V (off). These voltages are supplied by the interface box, and are fed through the filtering network shown in figure 3-2. The heat sinks each have an inductor and current limiting resistor going to ground to provide a DC return.

Because the output diodes at the antenna side of the tuning network must handle higher voltages and currents, they were biased more heavily. The output diodes were biased at 150 mA when on, and -100 V off; the input diodes were biased at 120 mA when on, and -100 V off.

Each of the six tuning networks provides a double-tuned impedance locus over the band. The components in each tuning network were carefully designed to minimize loss. Large inductors, characterized by the number of coil turns, were wound with 14 gauge wire in coils with inner diameters ranging from 0.35 to 0.50 inch. Adjacent coils were individually shielded to reduce inter-band coupling. Smaller inductors were made of a single turn of 12 gauge wire and were unshielded.

Because of the antenna transmit power requirements and operating frequency range, it was necessary to construct RF tuning coils in the above manner. These coils are all air wound to maximize the coil Q (which minimizes component power dissipation) and to keep the coil resonant frequency out of the operating band. Constructed coils had theoretical Q values ranging from 250 to 400. Chip RF tuning capacitors were purchased and, where required, several were connected in parallel to obtain the specified values. This reduced the circulating current flow in each individual chip capacitor during high power operation. The use of several capacitors in place of one reduced the component stress by reducing the power dissipated in each individual capacitor.

Considerable care was taken to minimize the power dissipated in tuning network components. Some problems were encountered with the 3.3-microhenry decoupling chokes. These were ferrite loaded inductors with a relatively low Q of 80. In many cases three chokes in series had to be used to avoid component damage under high power.

The lowest antenna efficiency is in the 30 to 33 MHz range. For 60 watts of input power, the component power dissipations have been computed and are listed in table 3-2.

Table 3-2. Power Dissipation in RF Tuning Network

Components	Power Dissipation, for 60 W Input
Input Forward Biased PIN Diode	0.25
Input (5) Reverse Biased PIN Diodes.	0.50
Shunt Double-Tuning Capacitor	1.00
Shunt Double-Tuning Inductor	2.60
Series Tuning Inductor	2.50
Shunt Tuning Inductor	2.50
Output (5) Reverse Biased PIN Diode	4.50
Output Forward Biased PIN Diode	1.35
DC Return Chokes (all)	1.60
Total Circuit Power Dissipation, W	16.80
Antenna Power Efficiency = -1.4 dB	

3.3 INTERFACE UNIT

The interface unit contains both the logic, which converts the ARC-114 frequency information to actual diode bias values, and the required dc power supplies. Figure 3-3 illustrates the interfaces between the aircraft, the interface unit, and the antenna. The interface unit receives +28 V from the aircraft, and three lines of voltages, representing the operating frequency, from the ARC-114. The frequency information is in 1-MHz increments. The interface unit supplies 11 lines of diode bias to the antenna.

The interface unit circuit is shown in figure 3-4. The inputs from the ARC-114 and aircraft power are shown on the left, the bias outputs are on the right.

Figure 3-5 shows the interior of the interface unit. The terminals which connect to the ARC-114 and the aircraft power are labeled.

The voltage steps from the ARC-114 are decoded using two digital quad comparator chips. The chips compare the ARC-114 voltage steps to a reference 15-V supply. The outputs of the chips are connected to a programmable logic array (PLA) chip. This chip provides design flexibility since the tuning bands can be easily changed. The chip

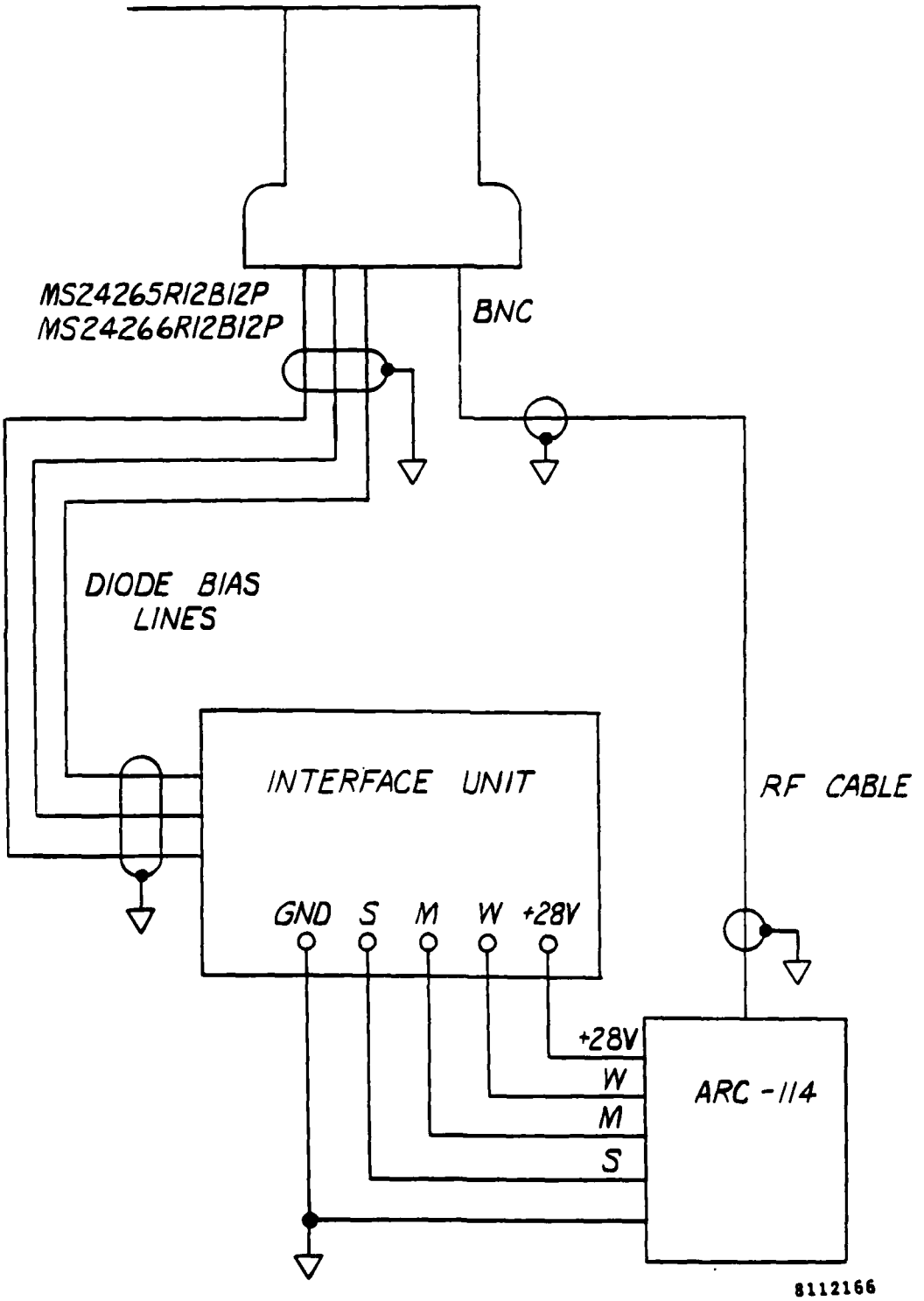

Figure 3-3. Zero dBi Antenna Interface Diagram

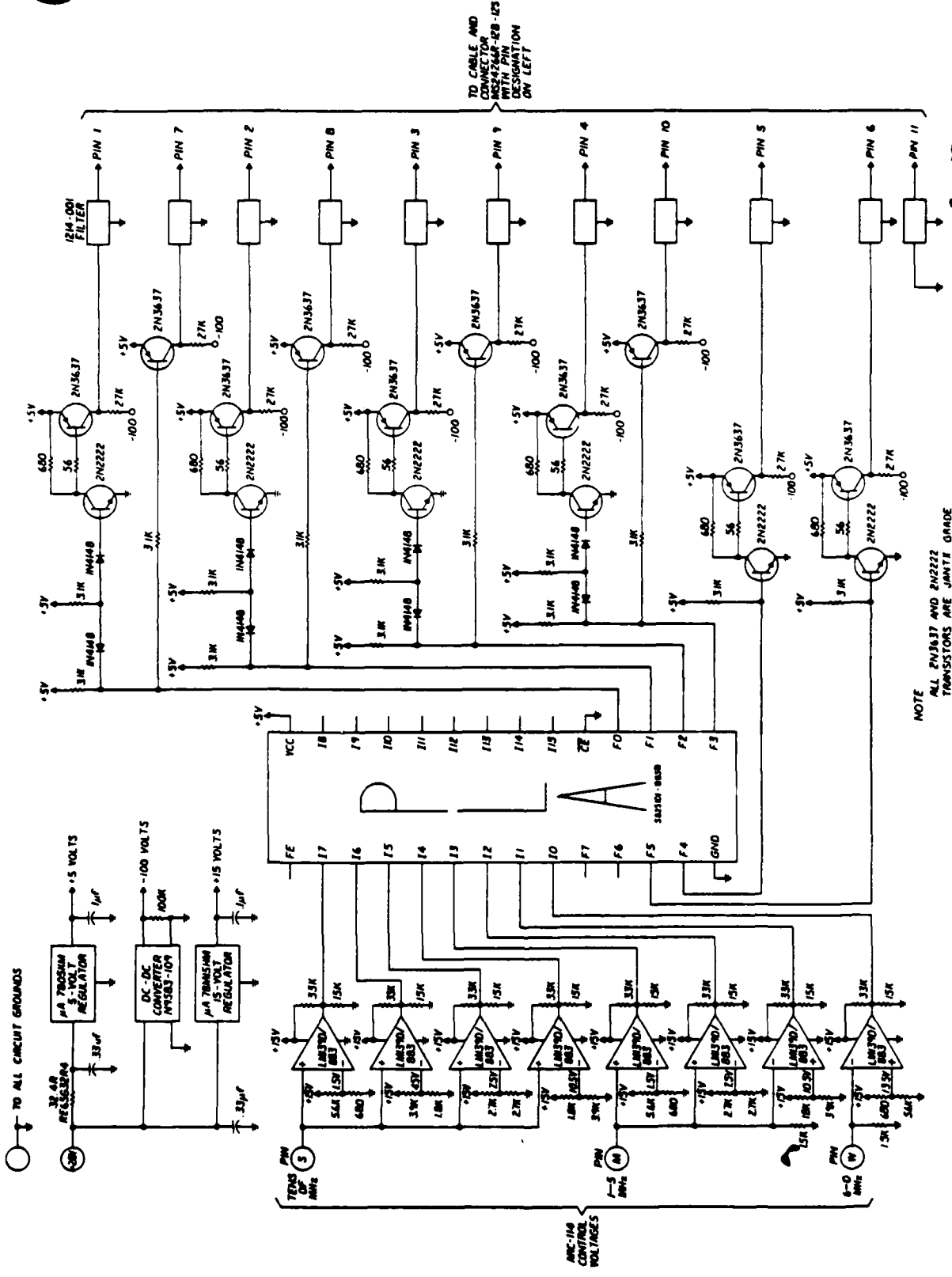

Figure 3-4. Interface Unit Schematic

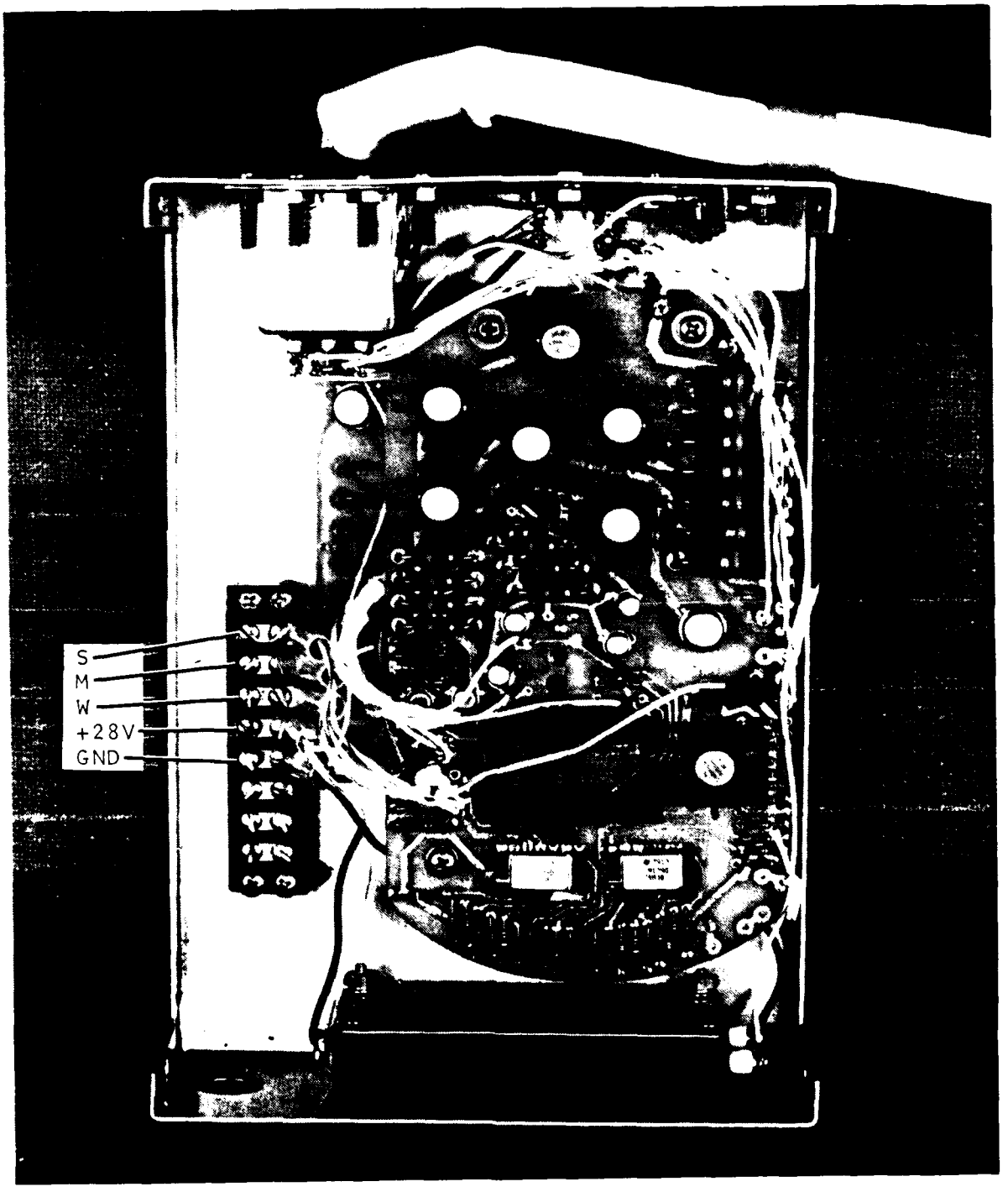

Figure 3-5. Interior of Interface Unit

determines which matching network is selected for a given frequency. By replacing this chip, different matching networks can be assigned to different bands. The chip is programmed using a special test jig.

The output of the PLA chip connects to the transistor drivers. One type of driver provides high current (300 mA) and another type low current (20 mA). The only difference between the two is the transistor 2N2222 pre-driver required for the high current design. In both drivers, transistor 2N3637 switches the diodes between +5 V and -100 V.

The ARC-114 supplies frequency information in the form of voltage steps in ARC-114 outputs from pins S, M, and W. The frequency versus pin voltage output is listed in table 3-3.

Note that the resistor used to limit the forward bias current is contained in the antenna. The driver works very simply. When the transistor is turned on, the diode is connected to +5 V, with the 27K ohm resistor preventing the -100 V supply from being short circuited. When the transistor is turned off, the current through the 27K ohm resistor is very small, and the diode line falls to -100 V.

Table 3-3. ARC-114 Interface

ARC-114 Connector Pins	Frequency, MHz	Output, V
S	30-35	3
	35-45	6
	45-55	9
	55-65	12
	65-75	15
M	1	3
	2	6
	3	9
	4	12
	5	15
W	6	3
	7	6
	8	9
	9	12
	0	15

The antenna switching time is dependent on the diode driver circuits. The diodes themselves have a time constant of 5 microseconds. The driver has an "on" time of less than 100 microseconds. In turning off the driver circuit, a 27K ohm, pulldown resistor is used to bias at -100 V. Additional bypass capacitance and filtering is added to the RF tuning circuits for EMI considerations, to assure reliable diode biasing. The total input capacitance is on the order of 0.05 uF, which in series with the 27K ohm resistor, results in a time constant of 1.35 milliseconds. In figure 3-6 a possible future modification to a typical bias circuit is outlined. The NPN high power transistors (Q_2) are placed across the 27K ohm pulldown resistors and coupled as shown. Transistor Q_1 and Q_3 switching will capacitively couple a pulse for just long enough to turn on transistors Q_2 and Q_4, and drain the current in the desired switching time.

This new circuit is analyzed below. As shown in figure 3-6 the input logical switch is either a short or an open circuit. For an open circuited input, at steady state conditions, and for a short circuited input, at initial circuit conditions, the component conditions are listed below:

Components	Open Circuited, Steady-State Conditions	Short Circuited, Initial Conditions
Transistor Q_1	On	Off
Capacitor C_1	+5 V	+5 V
Capacitor C_4	Uncharged	Uncharged
Transistor Q_2	Off	Off
Transistor Q_3	Off	On
Capacitor C_2	Uncharged	Uncharged
Capacitor C_3	-100 V	-100 V
Transistor Q_4	Off	Off

To meet the required switching time, capacitor C_1 must charge to -100 V and C_3 must charge to +5 V in less than 100 microseconds. Capacitor C_3 is charged quickly to +5 V by transistor Q_3. Transistor Q_1 is off, therefore, without Q_2, C_1 will charge with the time constant

$$\gamma = (0.05 \text{ uF})(27\text{K ohms}) = 1.35 \text{ millisecond.}$$

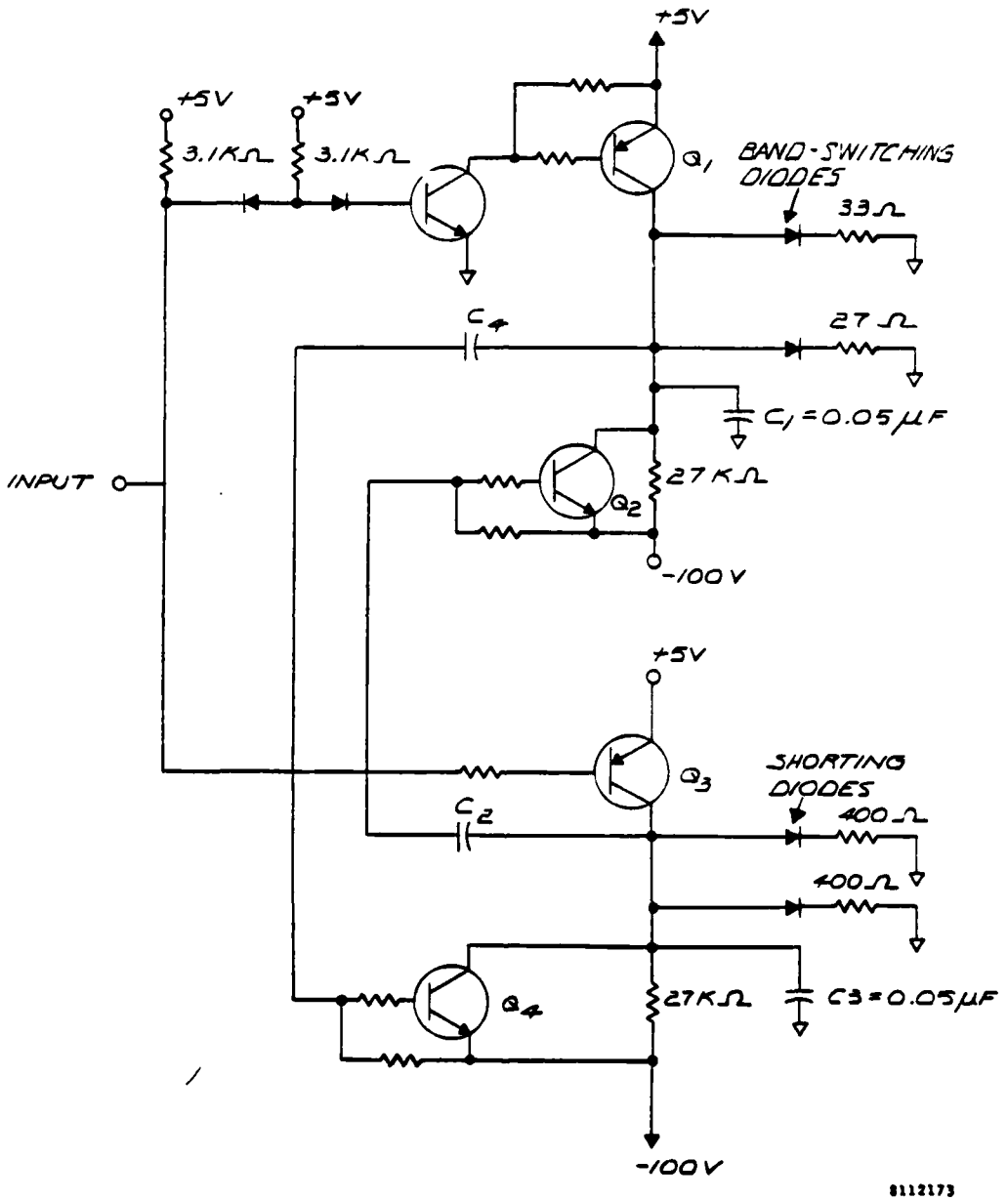

Figure 3-6. Modified Driver Circuit Design for Fast Switching

The equivalent circuit using Q_2 is shown in figure 3-7. Transistor Q_2 is turned on and must draw a current of CV/At or for C = 0.05 microseconds, V = 105 V, At = 10 microseconds, I_C = 0.5 A. The base current is (assuming β = 50) $I_B = I_C/\beta$ = 10 mA. Base current must then flow for 10 microseconds at 10 mA. Assuming C_2 does not charge past 50 V in 10 microseconds, the base current is I_B = 50/R, thus R = 5K ohms. Capacitor C_2 is selected such that the voltage across C_2 does not drop more than 50 V in 10 microseconds. The voltage across C_2 is: $V = 105e^{-t/RC}$, C_2 = 2.7 microfarads. Therefore, the swiching time can be reduced to 100 microseconds or less by the addition of extra driver transistors.

In summary, the logic and driver circuits are controlled and biased with the common ground connection and four voltages:

- o +28 V supply voltage
- o Pin S connection from ARC-114
- o Pin M connection from ARC-114
- o Pin W connection from ARC-114

The logic/diode bias draws a maximum of 0.7 A from the +28 V supply. Therefore, the maximum power consumption of the antenna and interface unit is 20 W.

3.4 MECHANICAL PACKAGING

3.4.1 Antenna Description

The zero dBi antenna was designed as a replacement for the FM 10-30-1 antenna and the Collins AS-2285 antenna. Thus the size, weight, and drag characteristics were tailored to approximate those of the existing antennas.

Figure 3-8 shows the antenna and its associated electronic interface unit. The antenna itself consists of two parts: the radiating element, and the RF tuning module.

The radiating element is constructed using a foam filled fiberglass shell. Copper sheet stock in the top of the antenna forms the radiator. The two top loading radials are fiberglass rods with axial wires inside.

The RF tuning module is mounted on the baseplate of the antenna. The unit connects to the antenna using a banana jack, as indicated in the photograph of the unassembled unit (figure 3-1). There are 12 screws used to fasten the base unit to the antenna fiberglass housing. In addition, three mounted heat radiators make contact with the diode heat-

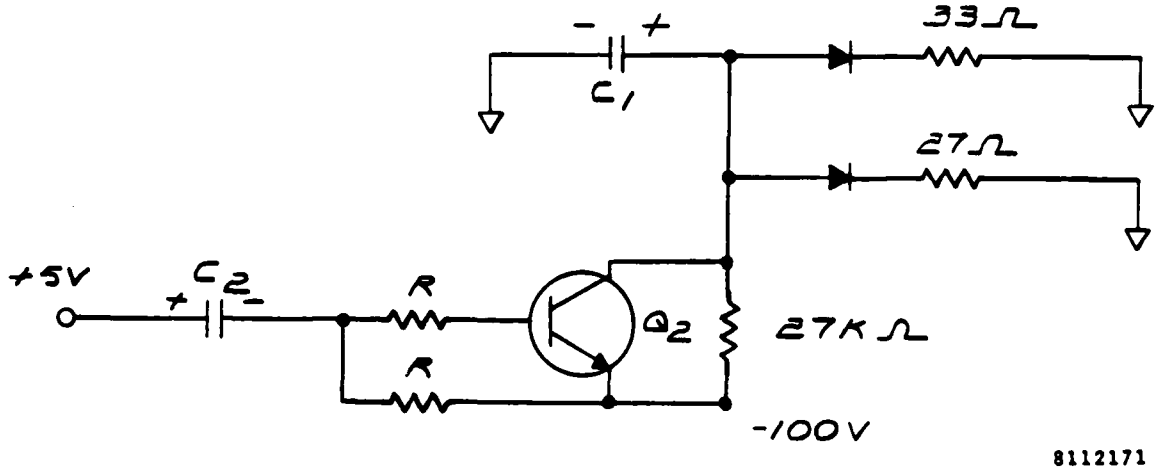

Figure 3-7. Equivalent Circuit using Q_2

Figure 3-8. Hazeltine's Zero dBi Antenna

sinks in the RF tuning module. It was necessary to provide this type of heat sinking for the diodes under high power conditions.

The RF matching components are mounted on two printed circuit boards. The inductors are foamed in their shields to provide resistance to shock and vibration. Other components are potted with a clear silicone RTV to provide vibration damping.

A shield is located below the two RF printed circuit boards. All diode bias lines are fed through low pass filters in the shield to assure that no VHF energy is propagated into the cable which runs between the antenna and the interface unit. The inside of the fiberglass housing is coated with conductive paint, and the shield completely encloses the bias connector and its associated wiring.

The dimensions of the interface unit, shown in figure 3-8, are 7 x 5 x 2.12 inches. The unit contains the logic and associated power supplies used to bias the switching diodes in the antenna. The heat sink shown in the figure is for the 5-V regulator. The interface unit contains two printed circuit boards; both are potted with a clear RTV to provide vibration isolation for the components.

The total weight of the radiator, including the tuning unit, is 4.5 lb; and the weight of the interface unit is 1.5 lb. The overall dimensions of the antenna are shown in figure 3-9.

3.4.2 Installation

Figure 3-9 shows the outline dimensions and the center of gravity of the antenna. With the exception of the two connectors, the zero dBi antenna uses the same mounting holes as the FM 10-30-1 antenna. The zero dBi antenna, of course, has a bias connector as well as a BNC RF connector. Because the BNC RF connector is not located on the centerline of the antenna, two new holes are required in the aircraft skin for installation.

Figure 3-8 shows the interface unit which may be installed anywhere in the aircraft. Since it must be connected to the ARC-114, the antenna, and the 28-V supply; a location which minimizes cable runs to those units is preferred. Figure 3-3 shows the interconnections of the antenna, the interface unit, and the aircraft equipment.

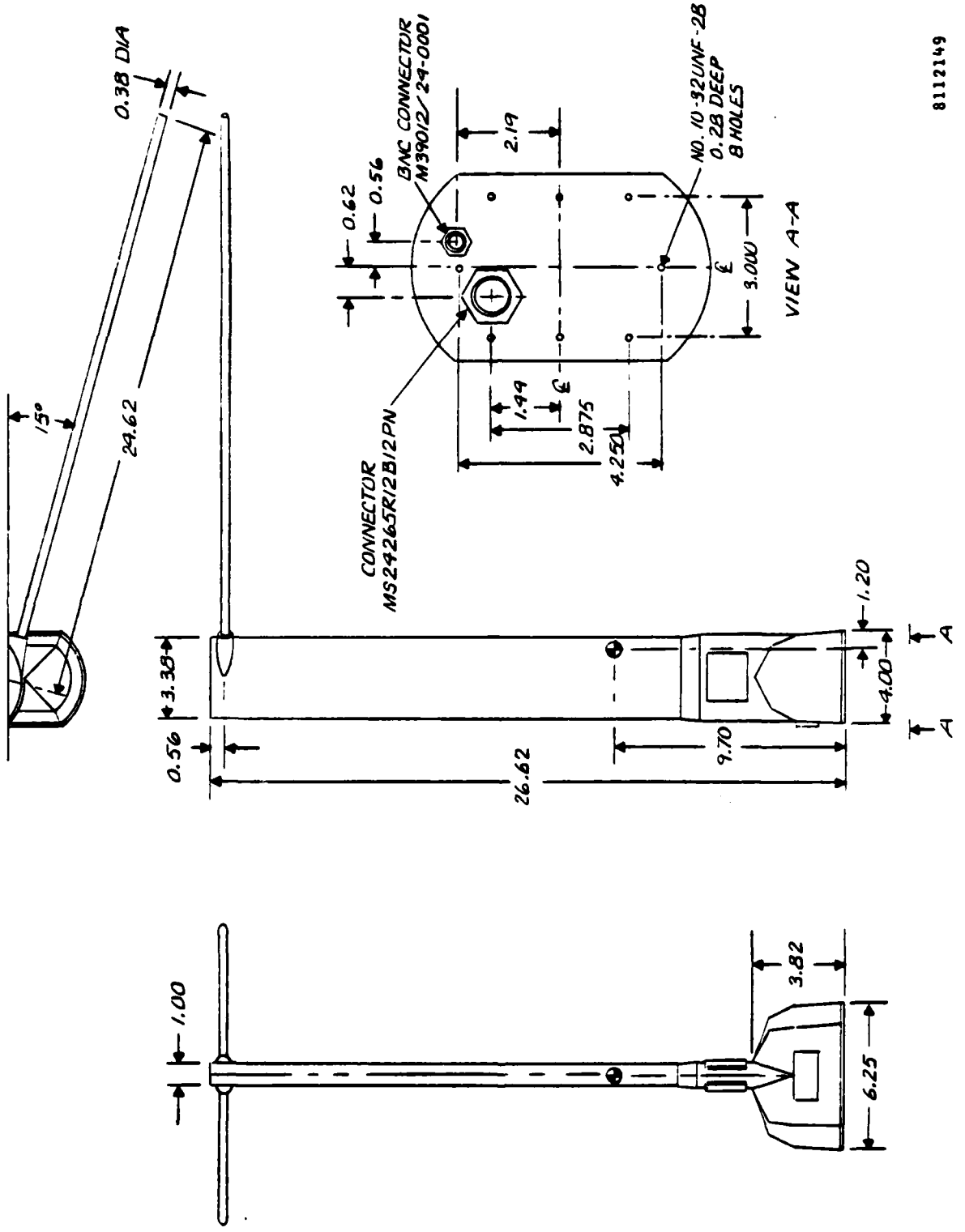

Figure 3-9. Zero dBi Antenna Outline Drawing

The location of the antenna on a particular airframe must be selected for best pattern coverage, taking into consideration the practical limitations of antenna height, available space, cable runs, etc.

For the OH-58A, the location shown in figure 3-10 was selected. This is the present location of the FM 10-30-1 antenna. The location offers good coverage, an existing RF cable run, and proximity to the ARC-114 radio.

Based on this location, a mechanical analysis of the installation was performed. Table 3-4 summarizes the results. Note that adequate margins of safety exist for all loads. The antenna resonant frequency and Q values also were measured (refer to Section 4); the measured values are in good agreement with those presented in table 3-4.

Table 3-4. Mechanical Analysis Summary

Mechanical Parameters	Results
Drag Loading	27.8 lb
Vibration Loading	34.5 lb
Shock Loading	135.0 lb
Antenna Blade Bending Stress	12,190 lb/in^2; MS=1.9
Maximum Mounting Bolt Stress	4,365 lb/in^2; MS-17.3
Antenna Blade Natural Frequency	21 Hz

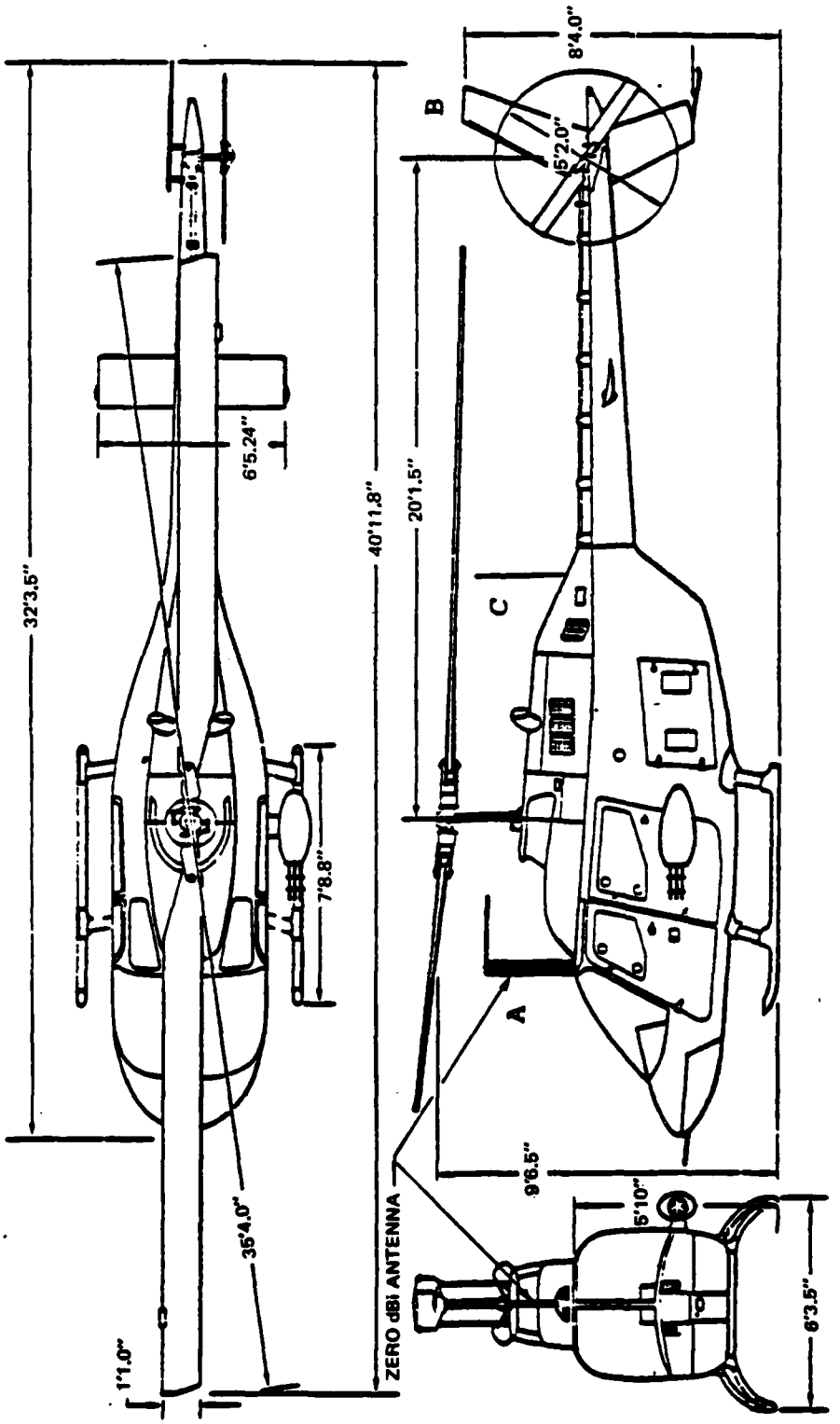

Figure 3-10. Zero dBi Antenna Installation on OH-58A

This page intentionally left blank

SECTION IV

TEST PROGRAM AND RESULTS

4.1 INTRODUCTION

During the course of the program, a variety of tests were made on the zero dBi antenna, ranging from diagnostic tests to the final acceptance tests. This section describes the test setups and the test results, and discusses significant variances from what was expected.

Subsection 4.2 describes the development testing performed on the prototype antenna. The results include measured patterns, gain on the OH-58A, and gain relative to some other existing helicopter antennas.

Subsection 4.3 discusses the factory qualification tests, including vibration, shock, and power capacity of a deliverable antenna.

Subsection 4.4 describes the results of acceptance tests performed on each deliverable antenna.

4.2 DEVELOPMENT TESTS

Many tests were performed on the prototype antenna to evaluate its performance against the design objectives. The most significant results obtained from these tests are summarized in this subsection. In some cases, such as power capacity measurements, tests on the deliverable units superceded earlier tests; in these cases the most recent results are presented.

4.2.1 Patterns

Both azimuth and elevation patterns of the prototype antenna were measured on a simple mockup located at Hazeltine's antenna facility located at Smithtown, New York. Because the airframe significantly influences the antenna pattern, these patterns are only an approximation to what would be expected on an airframe. Neither scale model nor full size measurements of an antenna mounted on an airframe have been made.

Figure 4-1 shows the test setup for the pattern tests. The mockup was positioned on a three-axis antenna mount. The mockup was, as shown, a rectangular box fabricated of wood and aluminum with dimensions of 15 x 8 ft. The antenna was

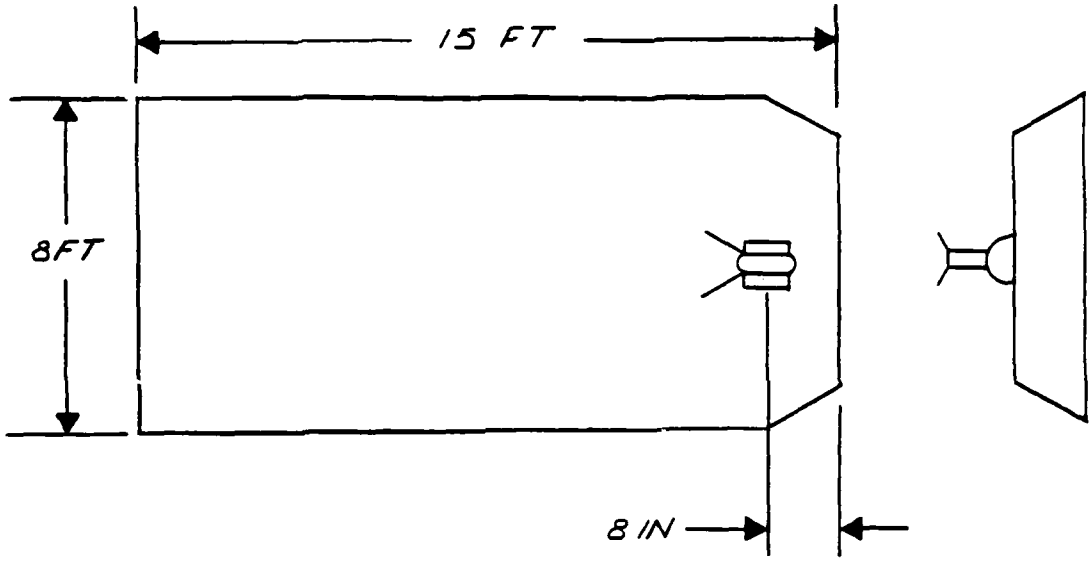

A) MOCKUP

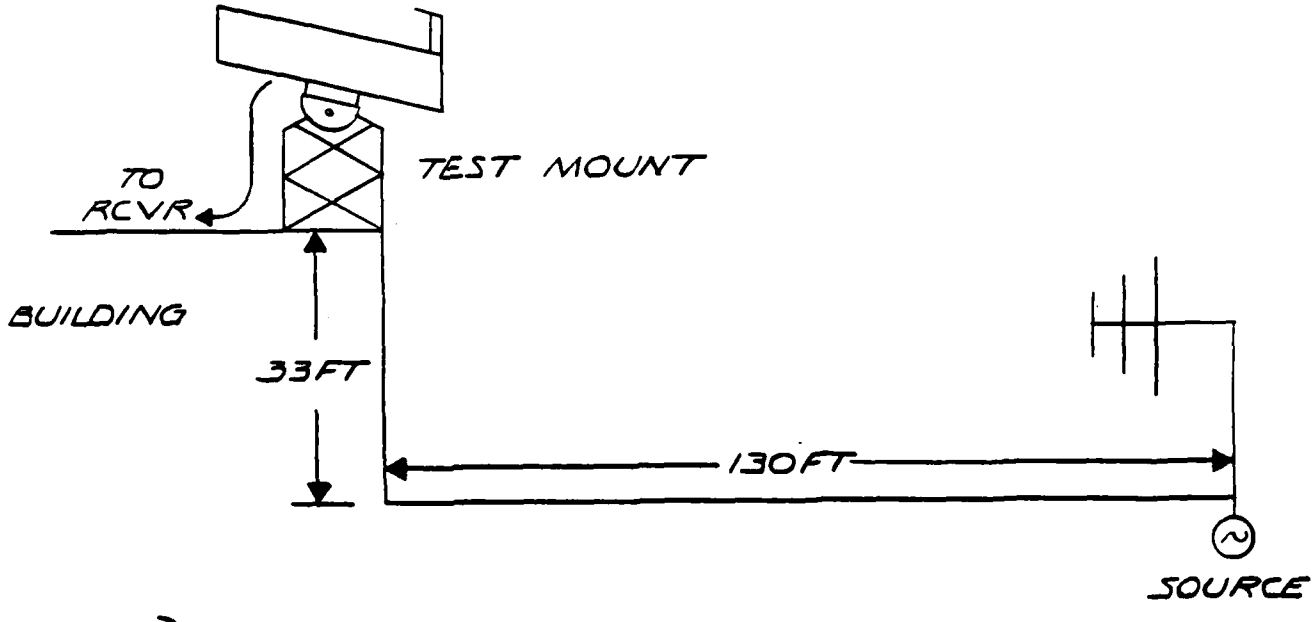

B) TEST RANGE

8112172

Figure 4-1. Antenna Test Setup

mounted on the forward edge of the mockup, approximately 8 inches in from the edge.

Azimuth patterns were taken at 20° elevation to verify that the pattern of the antenna is omnidirectional. The results are shown in figure 4-2. All plots are for 360° of azimuth, and have a vertical scale which is linear in dB with a 5-dB increment shown. At each frequency, the zero dBi antenna pattern response is plotted below the reference monopole pattern. There is no significance to the relative levels of the two patterns.

As can be seen, the patterns of the zero dBi antenna track those of the monopole rather closely, in most cases matching better than ±1 dB. The only significant exception is at 48.5 MHz, where the zero dBi antenna deviates by 3 dB from the monopole. The results show that the zero dBi antenna performs essentially as a monopole radiator.

Figure 4-3 shows the elevation paterns of the zero dBi antenna as a function of frequency. These patterns were measured at 0° azimuth using the same test setup as shown in figure 4-1, and they illustrate an important characteristic of the antenna/ground plane. For electrically small ground planes, the elevation pattern has a maximum at some point above the horizon. The location of the maximum depends on the size and shape of the ground plane, as well as the frequency of operation.

Note that the low frequency patterns, in general, have peaks at higher elevation angles. Thus, the loss of gain on the horizon is greater at lower frequencies. For example, at 31.5 MHz the difference between the elevation peak and the horizon is approximately 5 dB; at 88 MHz the difference is only 0.5 dB. A similar rolloff can be seen in the calculated pitch plane pattern of the VHF antenna on the OH-58A, as shown in figure 2-3. The impact of this pattern effect on the antenna is obvious - the high-angle pattern peak has maximum gain, and the gain at the horizon is reduced. This phenomenon is discussed further in subsection 4.2.2.

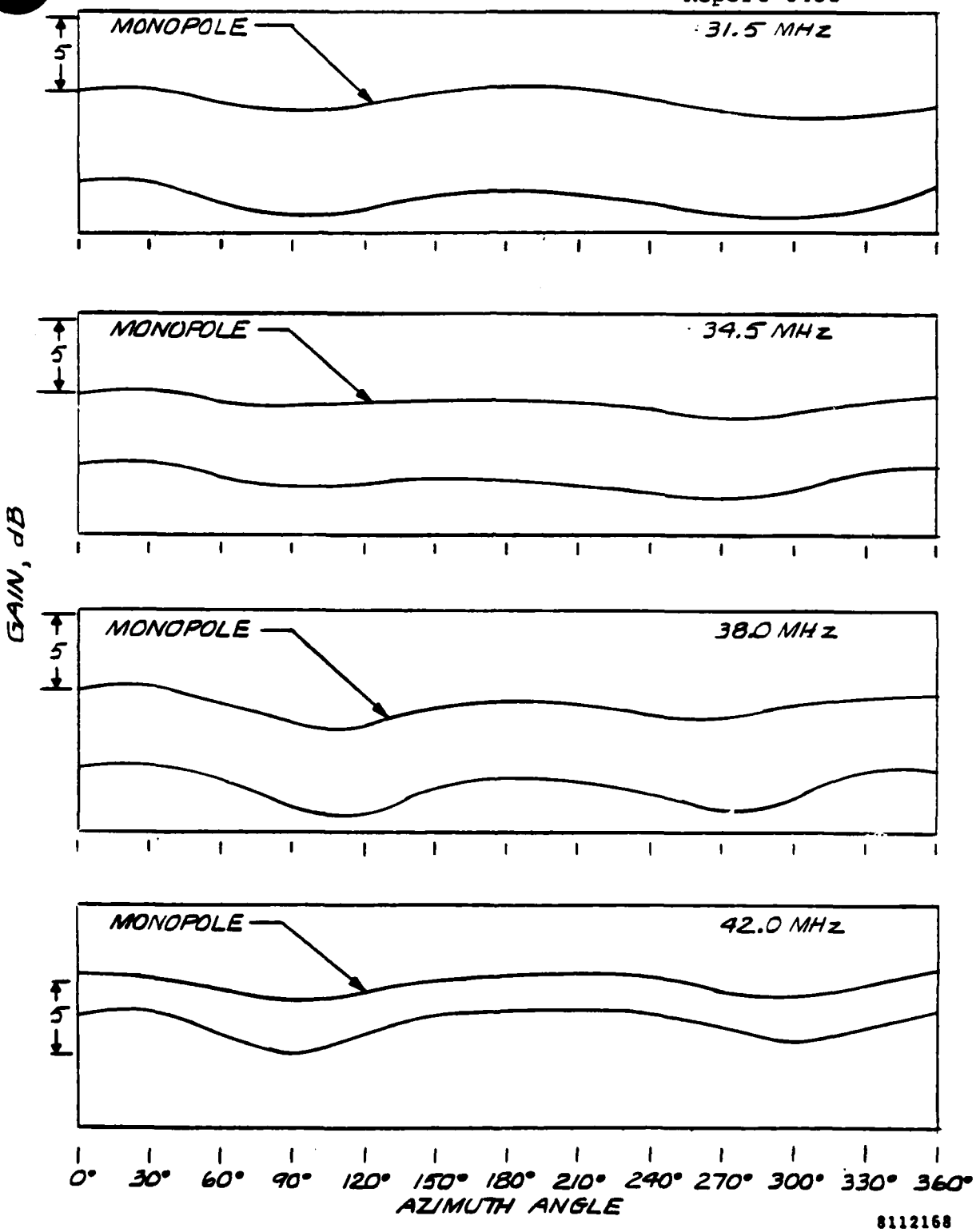

Figure 4-2. Zero dBi Antenna Measured Azimuth Patterns for 31.5 to 88.0 MHz (Sheet 1 of 2)

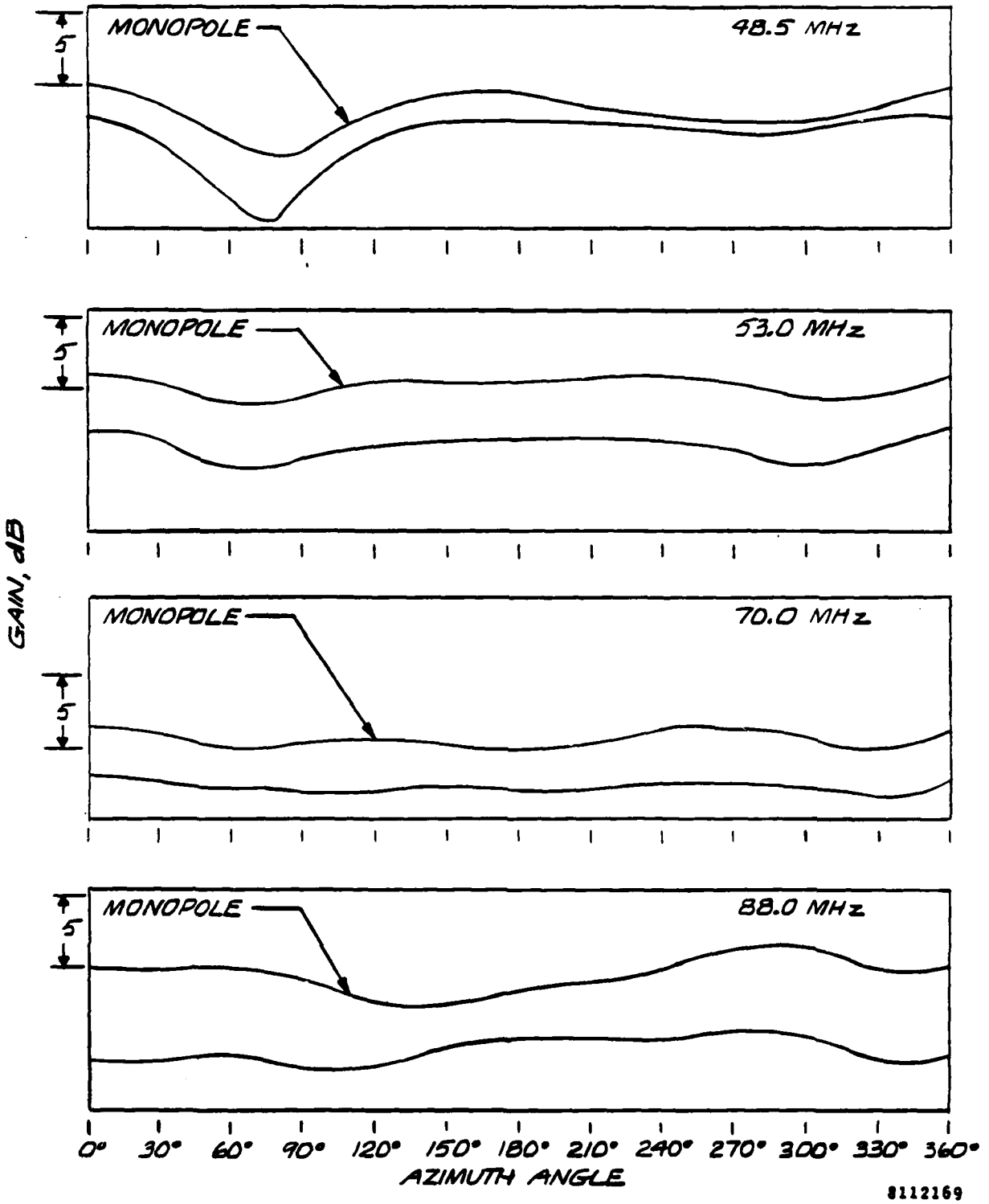

Figure 4-2. Zero dBi Antenna Measured Azimuth Patterns for 31.5 to 88.0 MHz (Sheet 2 of 2)

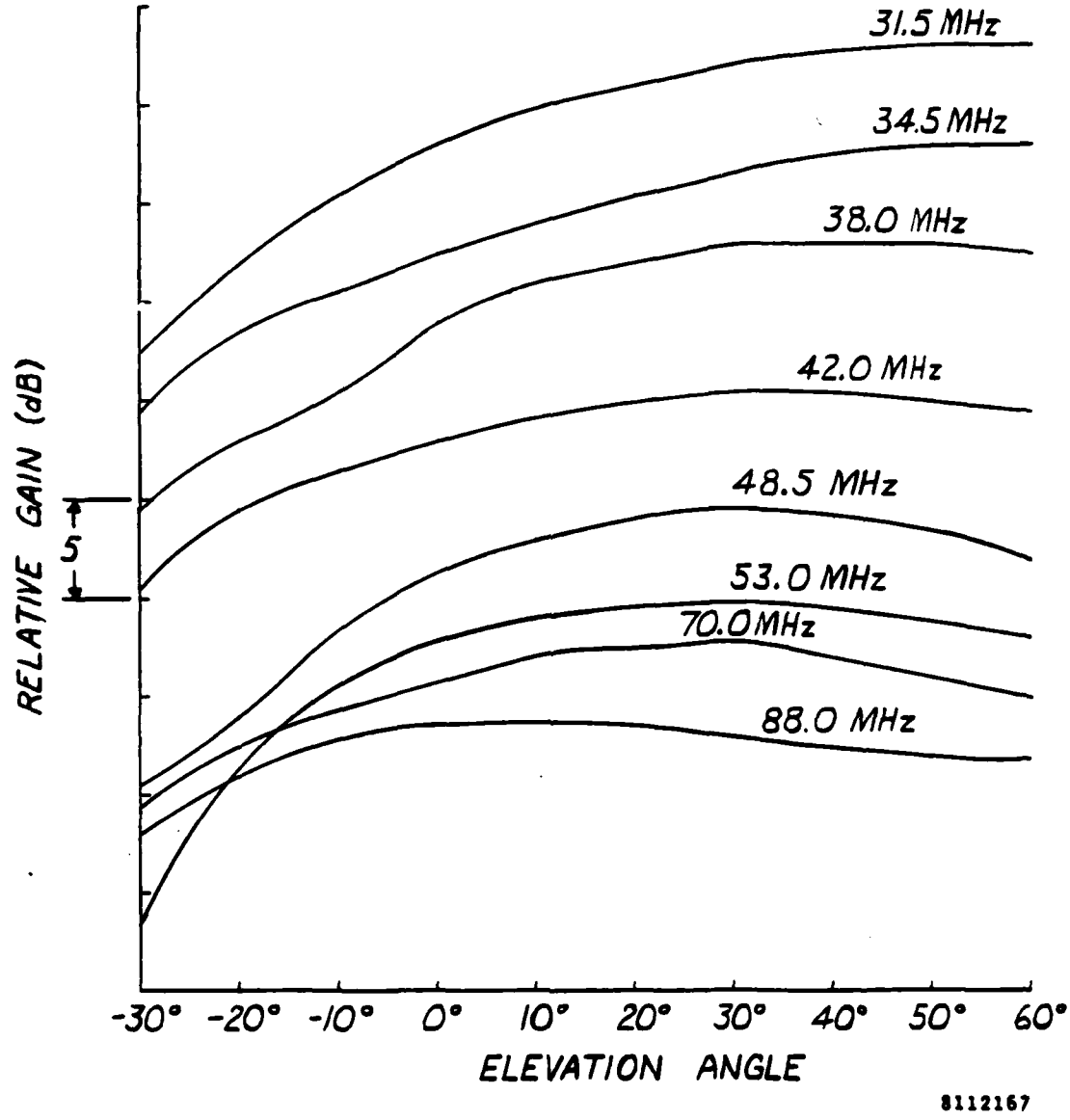

Figure 4-3. Zero dBi Antenna Elevation Patterns for 31.5 to 88.0 MHz

4.2.2 Gain

Several sets of gain measurements were made during development and final testing. Initial measurements were made with a prototype radiator mounted on an OH-58A. These tests were made in cooperation with AVRADA personnel, and used an OH-58A mounted on a pedestal, as shown in figure 4-4. Measurements were made relative to an adjustable vertical dipole mounted alongside, and at the same height as the prototype zero dBi antenna. The gain measurements were made off the nose of the helicopter and at approximately 0^{o} elevation. Measurements were made using a portable field strength meter.

The results of this initial set of measurements are shown in table 4-1. As expected, the lowest gain is at 30 MHz. This is a result of two factors: the rolloff of the elevation pattern, which is greatest at 30 MHz, and the higher losses in the matching components, which are a result of the low radiation resistance at 30 MHz. The low gain at 80 MHz is attributed to range effects, as it was not reproduced in further measurement.

To further evaluate these results, the same antenna was tested at Hazeltine's antenna test facility. The test setup shown in figure 4-1 was used. Here, a quarter-wave monopole was mounted on the same ground plane to serve as a reference. To avoid uncertainties concerning the gain of the monopole, its pattern was measured in several different cuts, then numerically integrated to derive the directivity. The resulting directivity was 2 dB. Note that this is considerably less than the theoretical gain of 5 dBi for a monopole mounted on an infinite ground plane. This is because the ground plane is so small that considerble radiation leaks around the edges, yielding a pattern more like a dipole than a monopole.

The gain of two other antennas was measured in the same location as the zero dBi antenna. One was an FM 10-30 "bent whip"; the other was an AS-2285 tunable blade.

Table 4-2 shows the results of the measurements on the horizon. Note that at virtually all frequencies, the gain of the zero dBi antenna exceeds that of the other elements by significant margins.

Table 4-3 shows the gain of each of the three antennas at their respective peak gains. Although the differences are not as pronounced as at the horizon, the zero dBi antenna outperforms the other two antennas, often by margins of 3 to 5 dB.

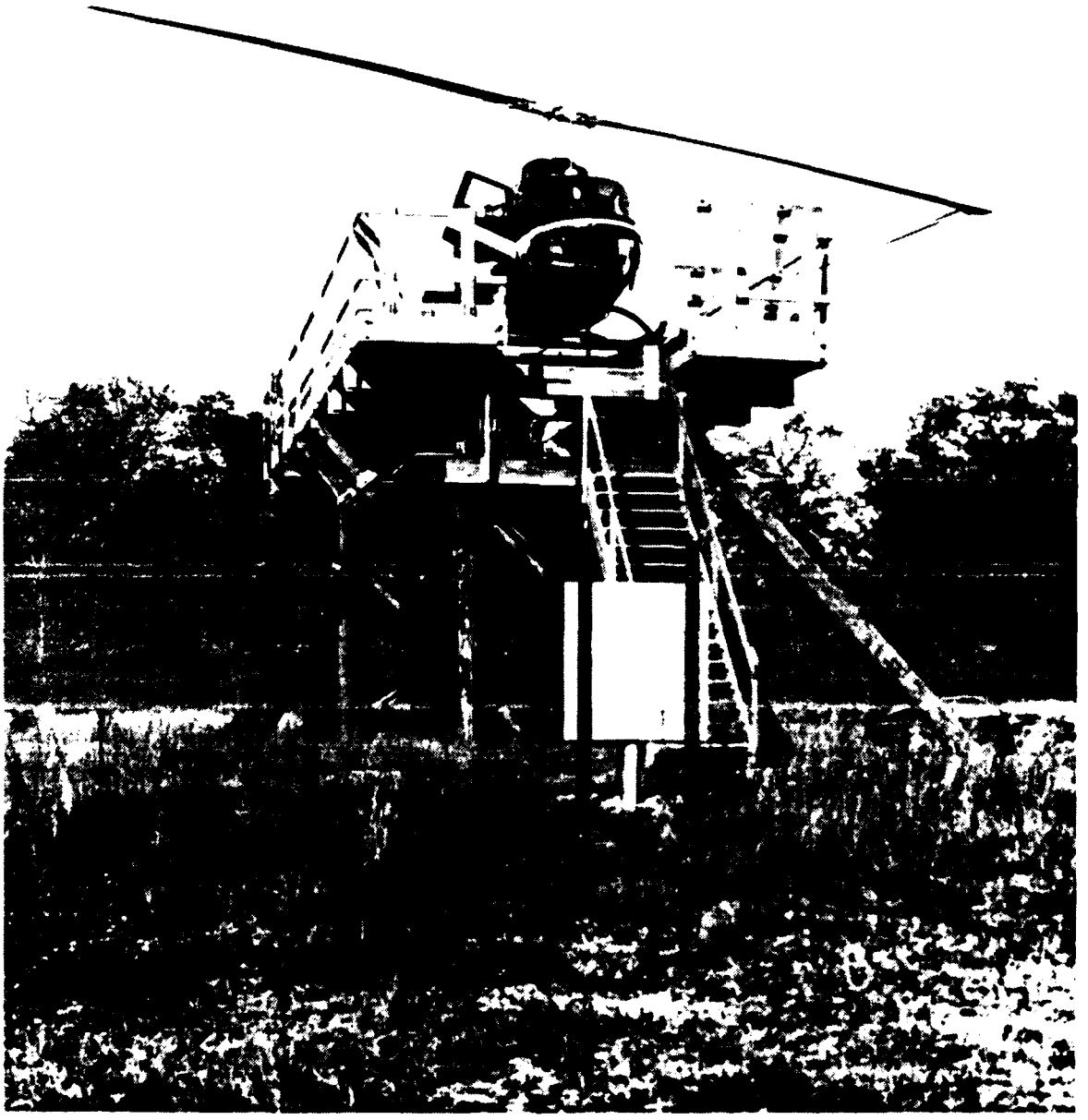

Figure 4-4. Zero dBi Antenna Undergoing Tests on OH-58A

Table 4-1. Measured Gain of Prototype Zero dBi Antenna

Frequency, MHz	Tuning Band	Antenna Gain, dBi
30.0	1	-8.50
32.0	1	-6.60
33.0	1	-6.33
33.0	2	-6.23
34.5	2	-5.12
36.0	2	-5.01
36.5	3	-6.94
38.0	3	-6.72
40.0	3	-4.03
40.0	4	-3.43
42.0	4	-1.75
43.0	4	-3.81
46.0	5	-2.40
49.0	5	+0.14
53.0	5	+0.21
60.0	6	-0.80
70.0	6	+1.44
80.0	6	-7.82

Note: Measurements made at Wayside, N.J. Measurements off helicopter at 0° Azimuth, 0° Elevation.

Table 4-2. Relative Gain of VHF Antennas

Frequency, MHz	Antenna Gain, dBi		
	Zero dBi Prototype	FM 10-30 Bent Whip	AS-2285 Blade
31.5	-4.5	-10.0	- 8.5
34.5	-4.0	-10.5	-11.0
38.0	-3.25	- 9.7	-10.25
42.0	-1.0	- 7.5	- 5.25
48.5	-1.25	- 6.0	- 5.75
53.0	-1.50	- 3.5	- 2.0
70.0	-1.50	- 5.7	- 0.25
75.0	--	--	--
88.0	-2.0	--	--

Note: Measurements at 0° Elevation, 0° Azimuth off end of ground plane.

Table 4-3. Relative Gain of VHF Antennas

Frequency, MHz	Antenna Gain, dBi		
	Zero dBi Prototype	FM 10-30 Bent Whip	AS-2285 Blade
31.5	0	-3.5	-2.0
34.5	+0.5	-4.0	-4.0
38.0	0	-5.5	-3.3
42.0	+0.75	-4.8	0
48.5	0	-2.5	-3.0
53.0	+0.75	-1.5	+1.5
70.0	+0.50	-3.5	+1.5
88.0	-1.5	--	--

Note: Measurement at 0° Azimuth, Peak Gain in Elevation

It is particularly important to note that the prototype antenna, which was used in these measurements, had significantly lower gain than the final five delivered units. Several components in the matching networks were changed during the final design tests on the deliverable units. These final units have 1 to 2 dB more gain than the prototype.

On the horizon, the measured gain is lower because of the shape of the elevation pattern. This additional loss varies between 1 and 5 dB, depending on frequency. Although the gain measurements on the ground plane used in these tests appears to agree with the measurements on the OH-58A, it would be worthwhile to investigate alternative mounting locations for the antenna. This could be done by measurement or calculation. The objective would be to select the location which maximizes the antenna gain on the horizon. Also, the patterns of the antenna on other airframes should be investigated. The sharp falloff in gain on the horizon is a result of the small size of the OH-58A. It is possible that a substantial improvement may be achieved on a large helicopter like the UH-1 or CH-47.

4.3 QUALIFICATION TESTS

There were no specific requirements for qualification tests in the contract; however, the antenna was subjected to limited vibration and shock testing to verify that the antenna would withstand the helicopter environment, and to power tests.

4.3.1 Vibration and Shock Tests

Vibration and shock tests were run on the prototype antenna, using Hazeltine facilities. The tests were performed in accordance with the test curves of MIL-STD-810C, method 514.2. Figure 4-5 shows the test curve as contained in MIL-STD-810C; the M curve was appropriate for the antenna.

Figure 4-6 shows the prototype antenna mounted on the vibration test fixture. The antenna was vibrated in three axes, with a sweep from 15 to 2000 Hz performed to identify structural resonances. Then, the antenna was vibrated for one-half hour in each axis, dwelling on the strongest structural resonance.

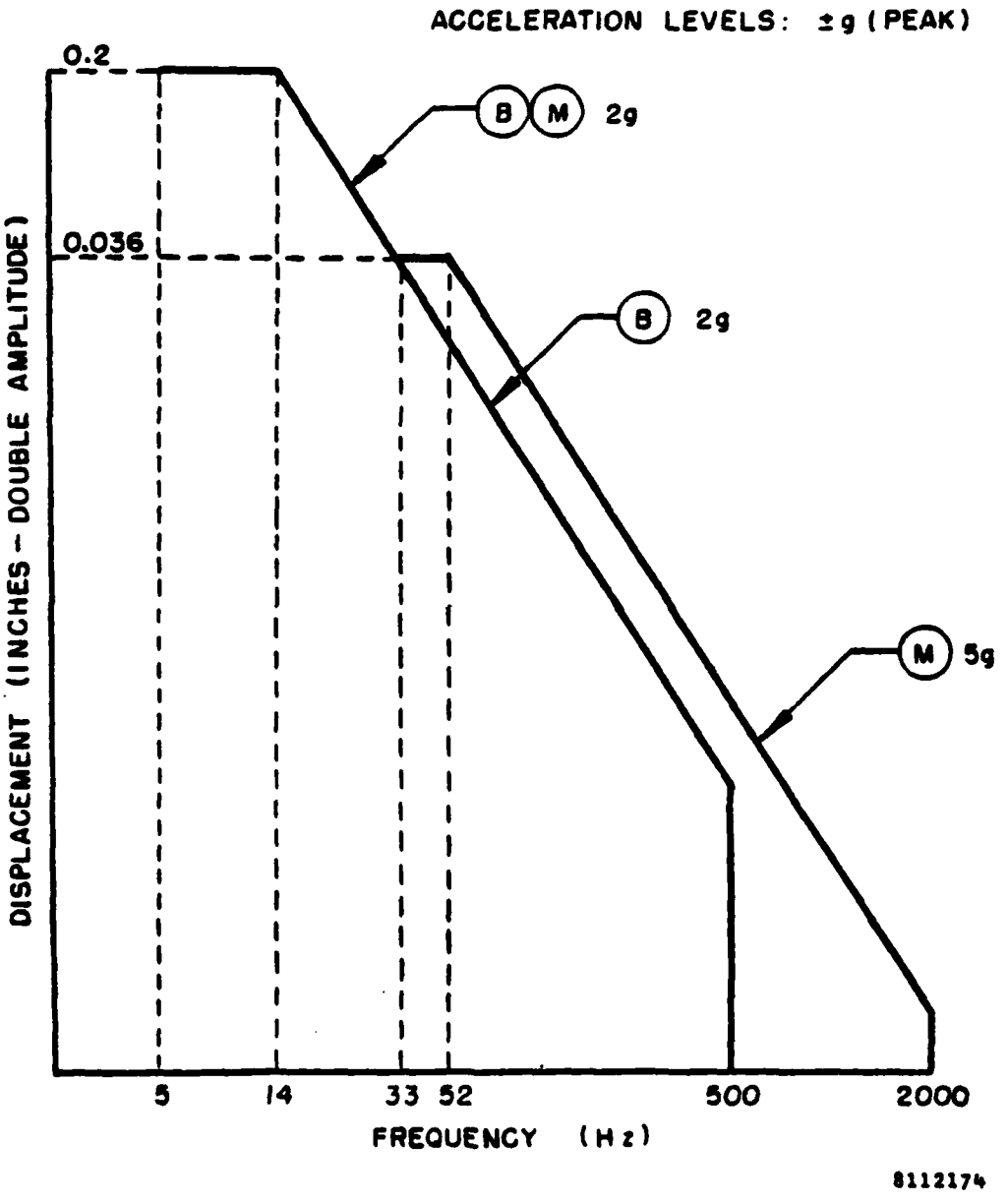

Figure 4-5. Vibration Test Curves for Equipment Installed in Helicopters, Equipment Category c

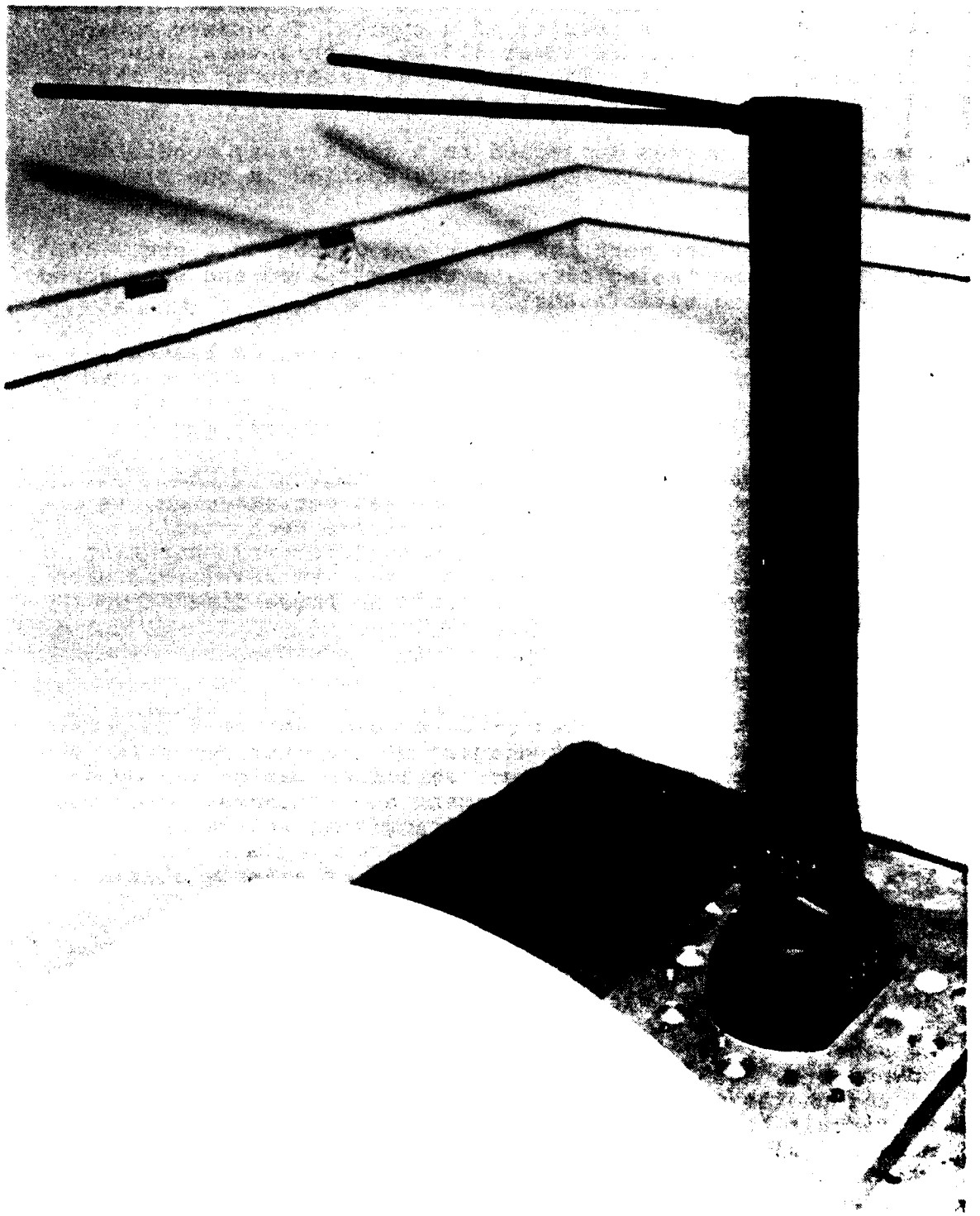

Figure 4-6. Prototype Antenna Undergoing Vibration Testing

Figure 4-7 shows the results of a typical frequency sweep. The strongest resonance is at 510 Hz, with several other secondary resonances. The structural resonances and the Q of the resonance agreed well with calculations.

The antenna also was subjected to a shock test, consisting of a 20-g shock for 11 milliseconds applied in one plane (forward-aft).

The antenna passed both the shock and vibration tests. All the digital and tuning circuits were retested and were found to be operating satisfactorily.

One minor discrepancy was noted after vibration testing. The fiberglass housing of the prototype antenna developed some surface stress cracks at the junction between the vertical portion of the antenna and the housing for the matching circuits. These stress cracks were in a surface layer which had a high resin-to-glass content. The structural integrity of the antenna was not affected, as demonstrated by the lack of change in its mechanical resonant frequency. To assure the satisfactory operation of the deliverable antennas, this junction was reinforced with additional layers of resin and glass in these final five antennas.

4.3.2 Power Tests

One of the five deliverable antennas was subjected to power capacity testing. A block diagram of the test setup is shown in figure 4-8. The power amplifier was driven by an H/P 608 signal generator. Incident and reflected power was monitored with a Bird Model 43 directional wattmeter.

The antenna was mounted near the edges of a large aluminum mockup, located 3 feet above ground level.

All power tests were run with 60 watts average power. The peak power capacity of the antenna was verified by the application of 100 watts for a short period (a few seconds).

Average power testing revealed two problems: some lossy components, and interference with the digital logic. Some of the chokes used to decouple the diode bias lines to the RF circuit had to be replaced with larger values. Also, some additional shielding and filtering was added to eliminate EMI to the digital logic.

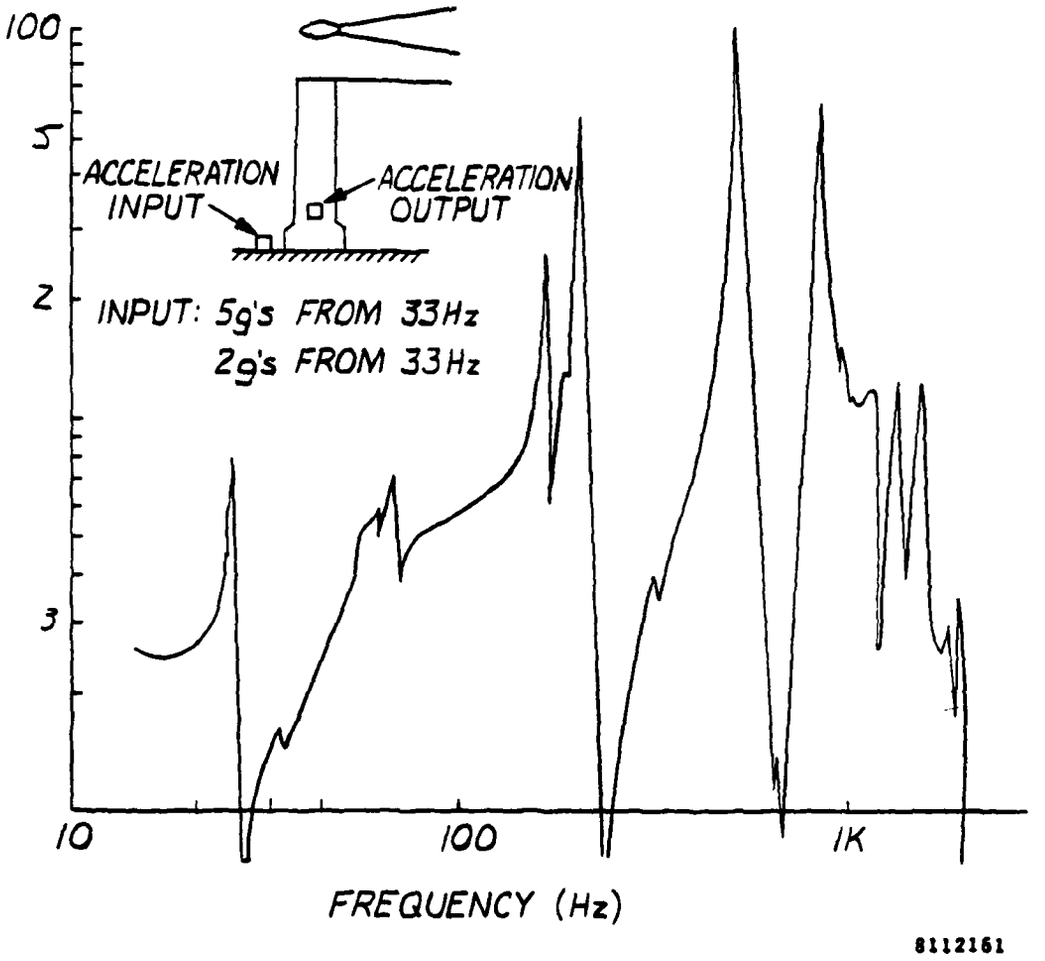

Figure 4-7. Actual Vibration Plot in Horizontal Axis

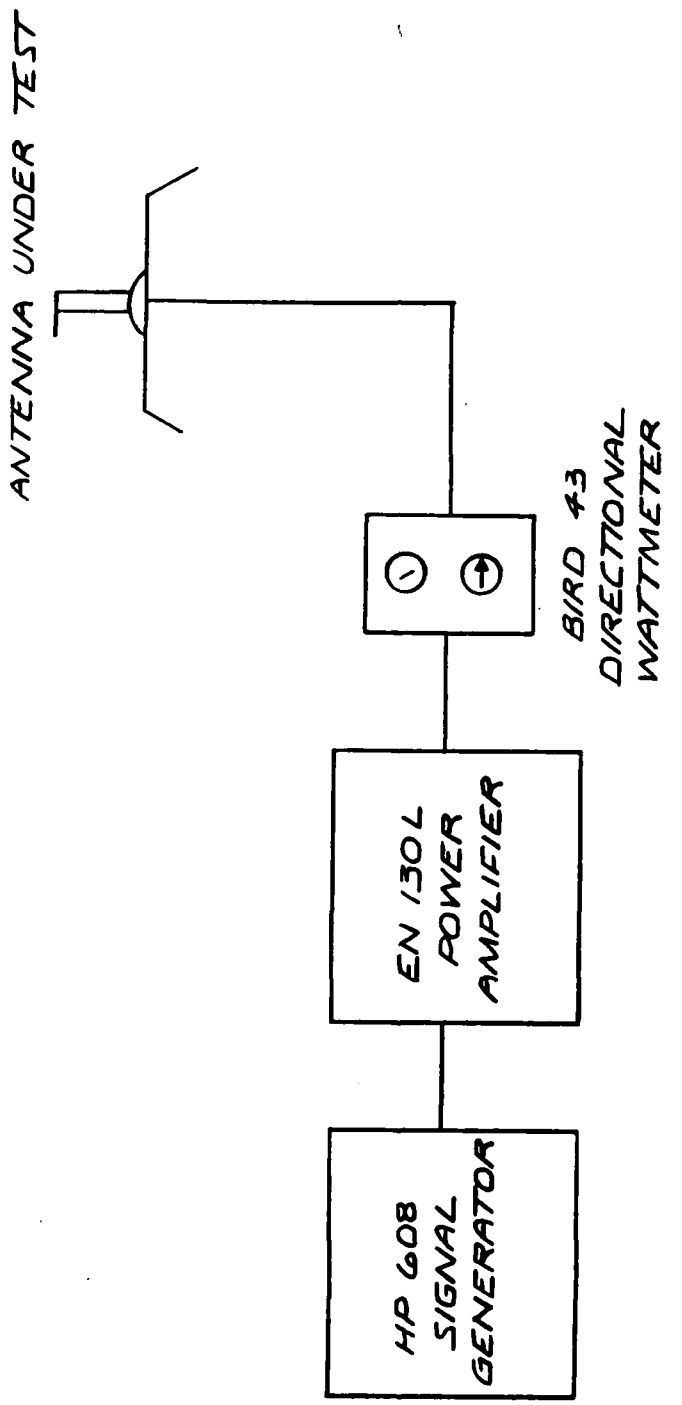

Figure 4-8. Power Test Setup

Final tests on the antenna consisted of operating the antenna for 5 minutes at 60 watts input to each band. The reflected power was monitored continuously to verify that no change, indicating a component breakdown, occurred. In operating the antenna, it is recommended that continuous power levels of 60 watts be limited to 5 minutes because the antenna performance has not been verified for longer periods. The antenna is intended to handle peak powers of 110 watts as produced by two 30-watt transmitters combined. It is recommended that the antenna not be exposed to continuous power of 110 watts for longer than a few seconds.

4.4 ACCEPTANCE TESTS

All deliverable antennas were subjected to a burn-in period and then acceptance tests.

The burn-in consisted of an initial vibration test and a 24-hour burn-in of electrical components. The burn-in test consisted of a 1-hour swept frequency vibration test. The antenna was driven in the roll plane, and the vibration was 1.5 g over a frequency range of 15 to 2000 Hz.

Electrical burn-in consisted of operating the diodes and their associated drivers for 24 hours.

At the completion of the burn-in tests, the antennas were tested for power capacity and impedance. The power capacity was tested using the test setup previously described. Each band was tested for 1 minute at 60 watts incident power.

Finally, the impedance of each antenna was measured for each tuning band. This verified that both the digital logic and the matching networks were functioning properly. Figures 4-9 through 4-14 show the measured impedance for one of the five antennas. Approximately 70% of the frequencies in the 30 to 88 MHz band are matched to within a 2 to 1 VSWR; the balance of the frequencies are matched to within a 3 to 1 VSWR.

It can be seen from the impedance plots that some bands are matched better than others, thus further design effort could improve the overall VSWR. It is estimated that a reallocation of the frequencies in each band, and some modification of the matching circuits, could reduce the VSWR at all frequencies to less than a 2.5 to 1 VSWR. If a seventh band were added, along with the revisions to the logic and matching networks, a 2 to 1 VSWR could be achieved.

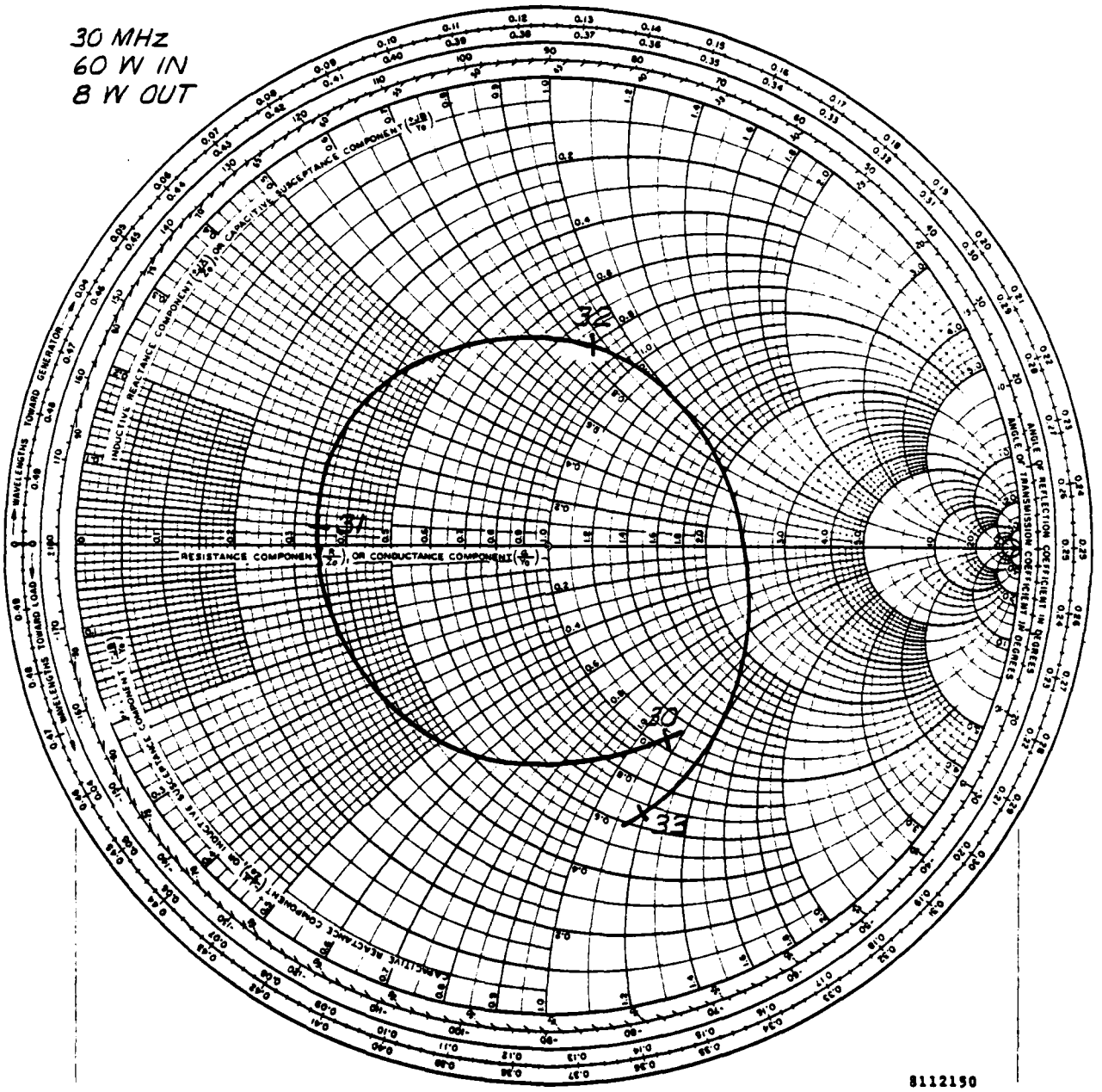

Figure 4-9. Measured Impedance Locus, Band 1

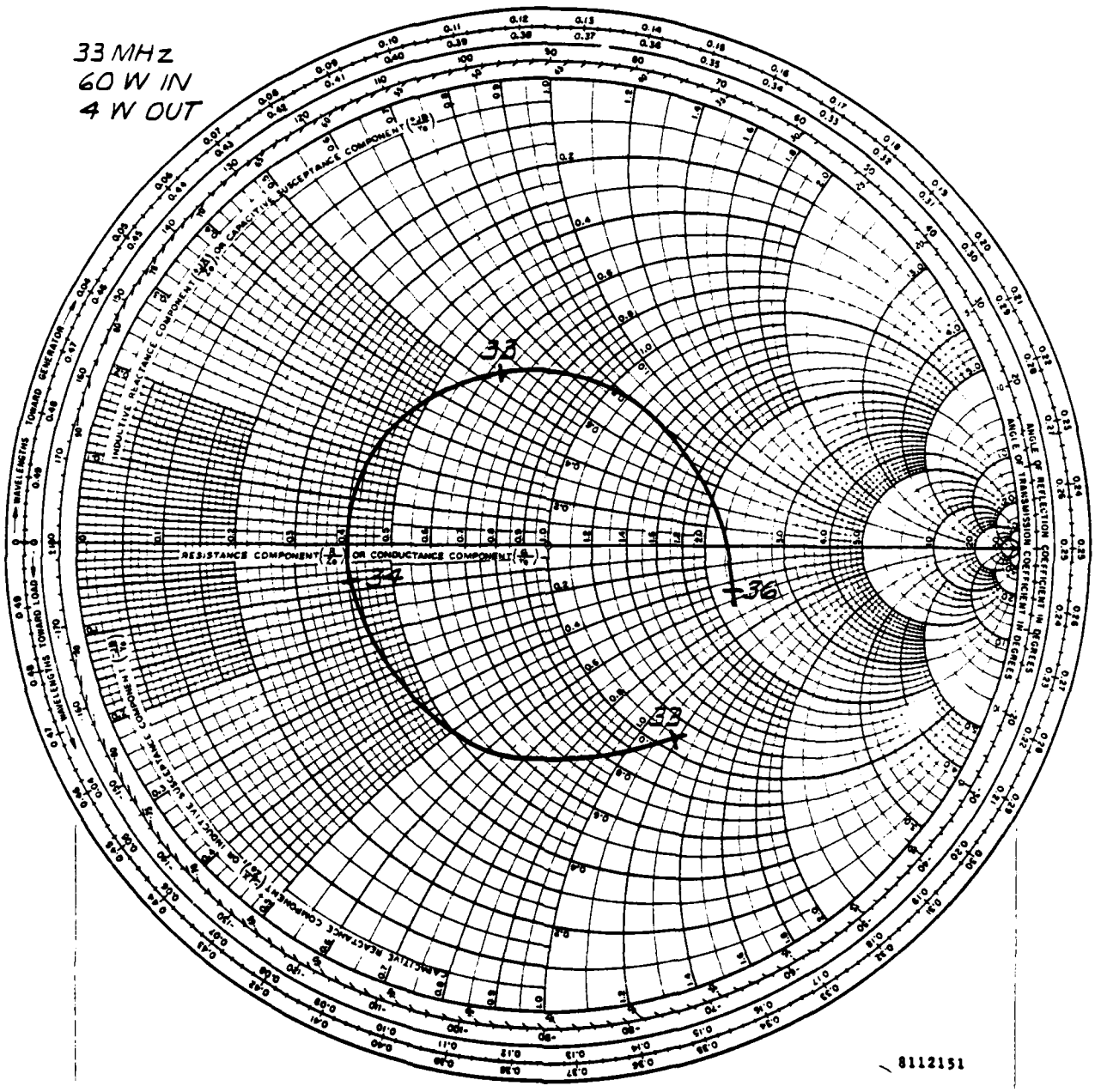

Figure 4-10. Measured Impedance Locus, Band 2

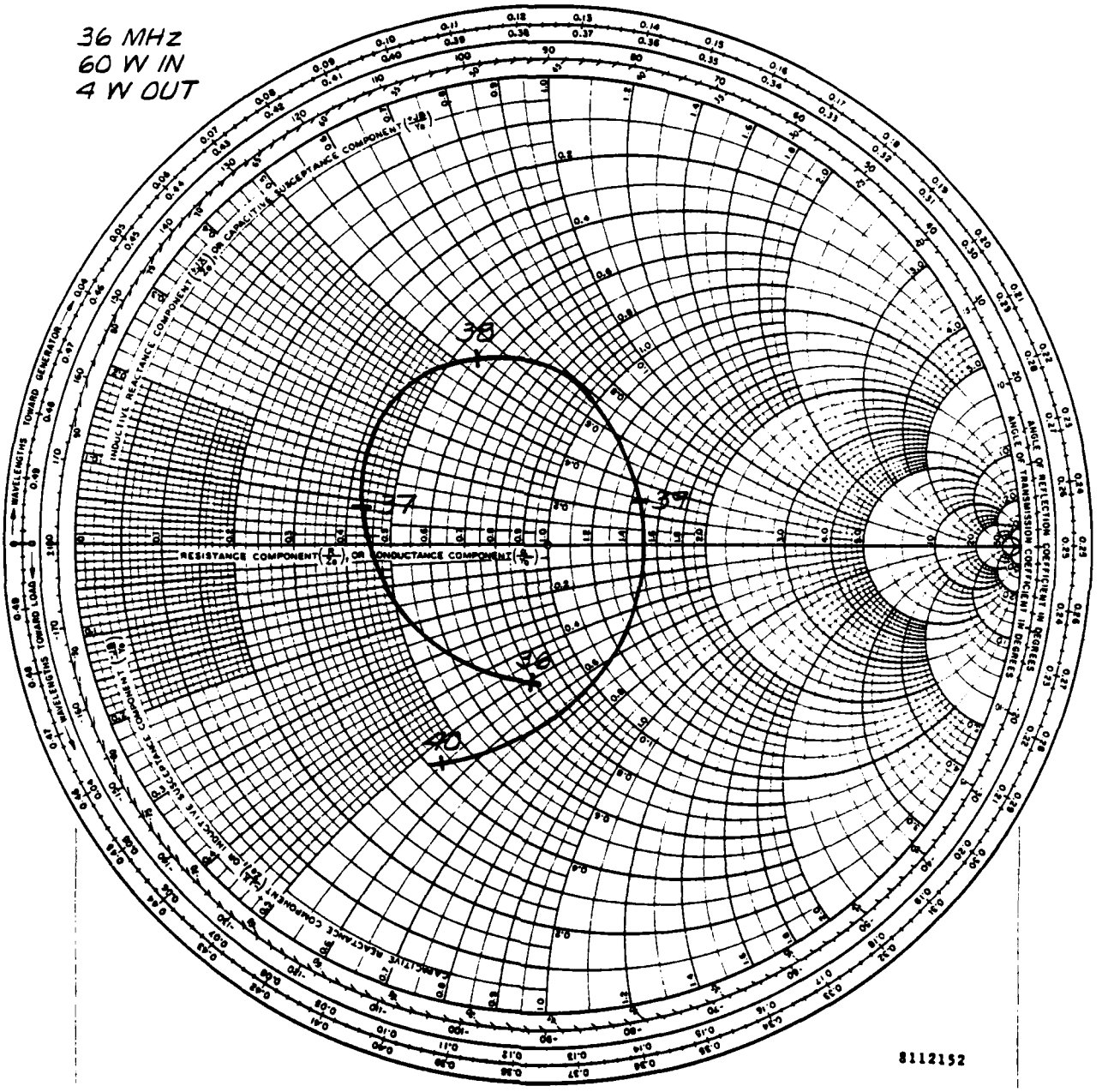

Figure 4-11. Measured Impedance Locus, Band 3

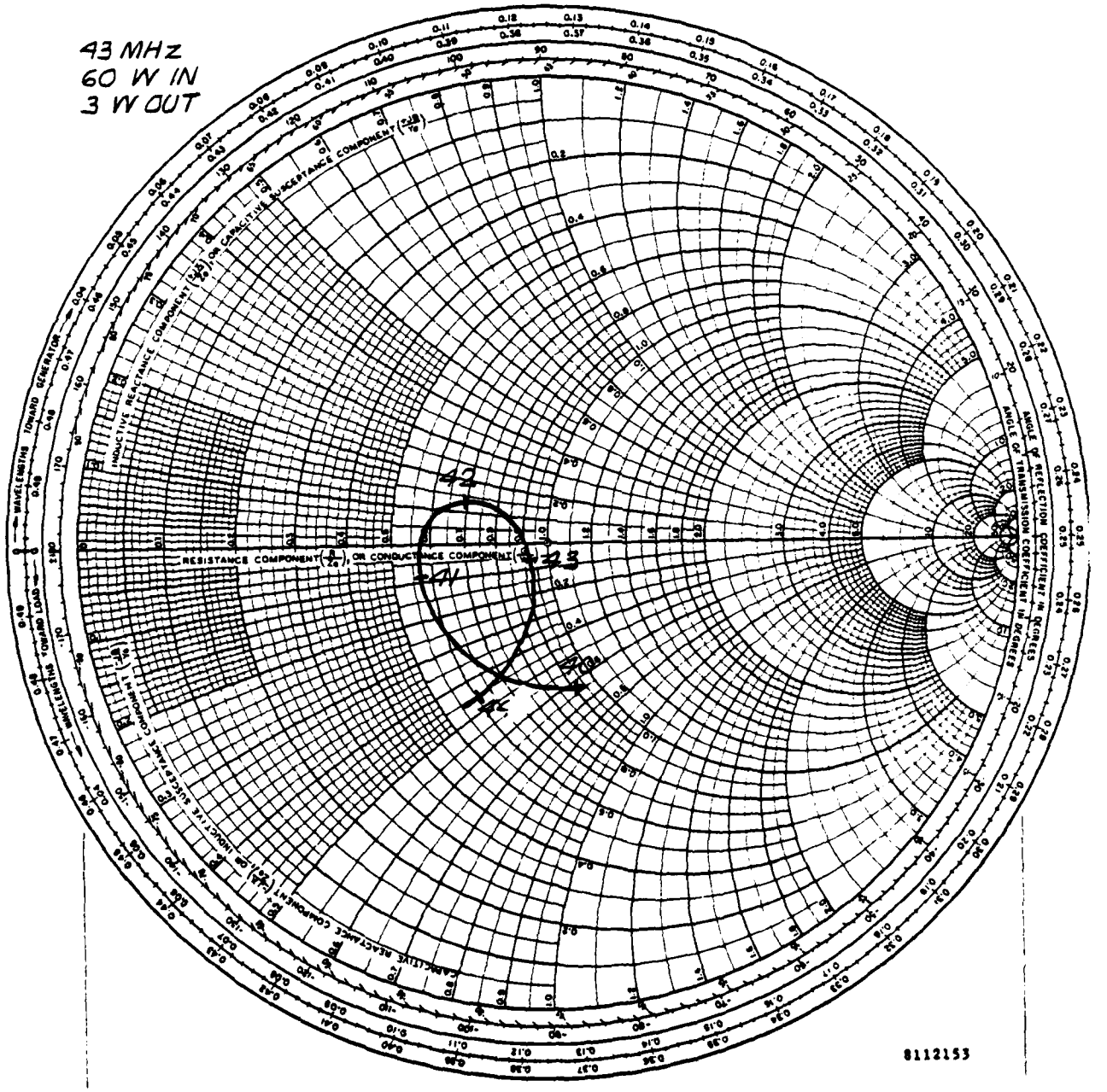

Figure 4-12. Measured Impedance Locus, Band 4

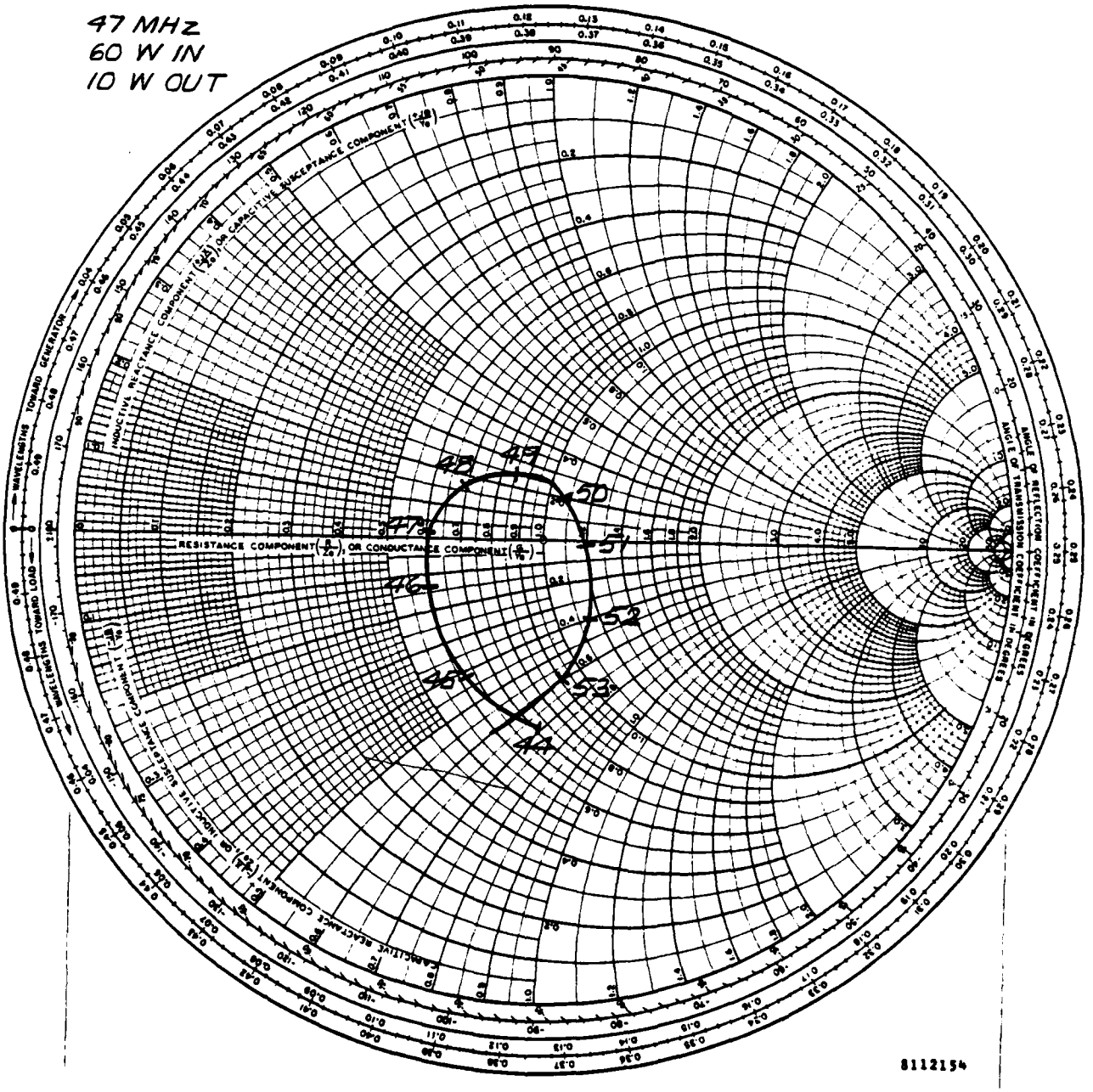

Figure 4-13. Measured Impedance Locus, Band 5

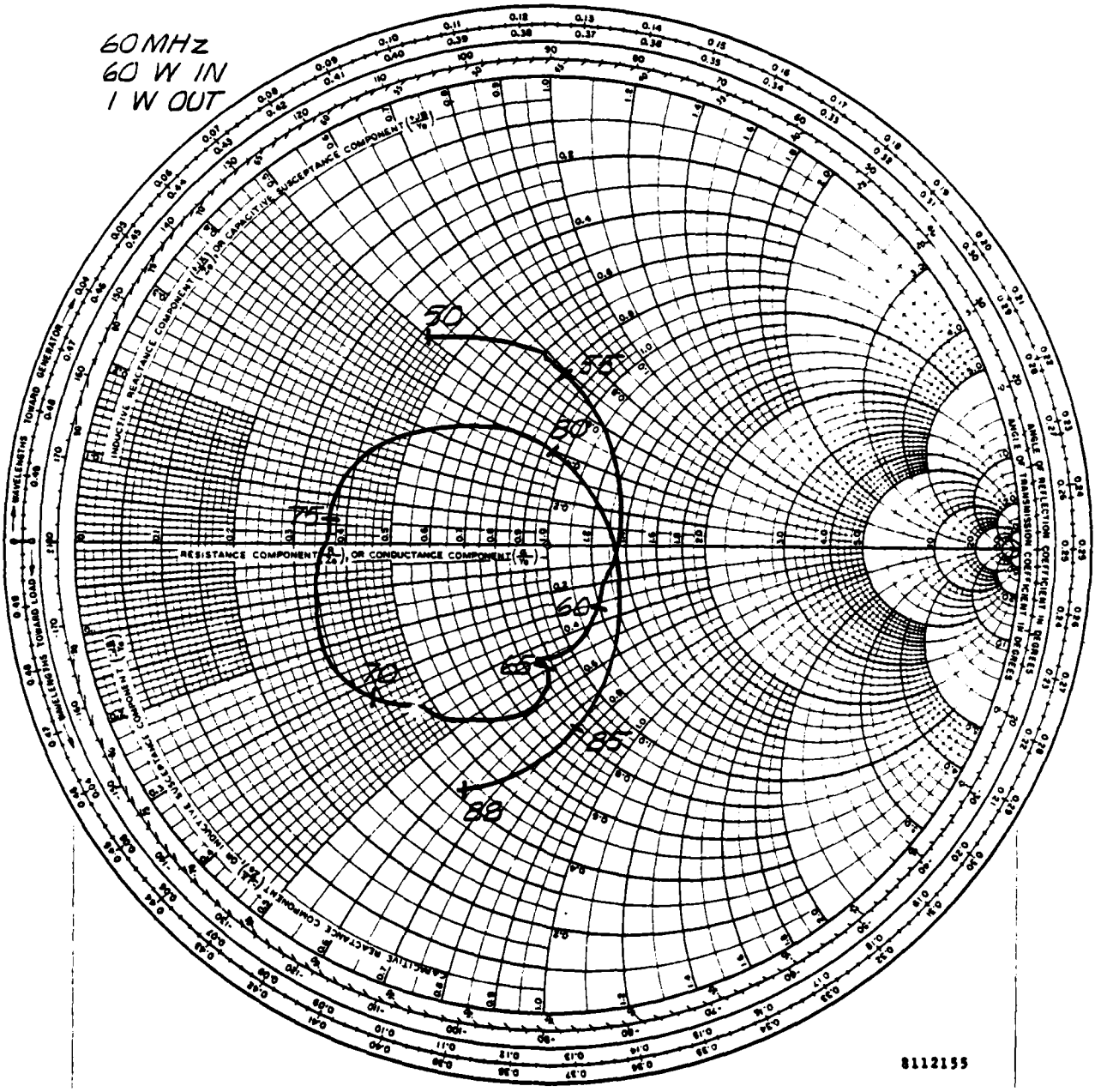

Figure 4-14. Measured Impedance Locus, Band 6

SECTION V

SUMMARY, CONCLUSIONS, AND ACKNOWLEDGEMENTS

5.1 SUMMARY

The results of this development demonstrated an electrically small, high efficiency antenna. The zero dBi antenna is the first known VHF antenna to utilize PIN diodes for switching, to achieve fast tuning with high power capacity.

Table 5-1 summarizes the measured performance of the antenna compared to the initial design objectives. The major objective of the effort, an antenna with zero dBi gain, was achieved. This makes the antenna the highest gain radiator available for airborne VHF-FM.

The tests showed that the antenna met five of the initial eight design objectives. The antenna did not meet three of the design objectives: VSWR, gain at the horizon, and switching time; and of these, VSWR and switching time can be made to meet the objectives with a modest additional design effort. The reduced gain at the horizon is a more fundamental problem which requires more analysis. A search for alternative antenna locations or radiating elements would be necessary to reach a conclusion on whether this objective can be met.

5.2 CONCLUSIONS

The antenna demonstrates that a high gain, fast tuning antenna is feasible. Hazeltine's conclusions, based upon the results of this development, are:

- Fast tuning VHF antennas using diode switches are practical. It is recognized that these designs will cost more than a simple whip antenna.
- Airframe pattern effects present a fundamental limit on achievable horizon gain. Future studies must address this problem.
- The open loop tuning system that was designed during this effort may not be optimum for all aircraft. Some deterioration of the VSWR is bound to occur when the antenna is mounted on other airframes; therefore, alternative tuning methods should be investigated.

Table 5-1. Zero dBi Antenna Performance

Parameter	Design Goal	Measured Performance
Frequency Range	30 to 88 MHz	30 to 88 MHz
Gain	0 dBi	+0.3 to +2.5 dBi (1) -4.8 to +0.3 dBi (2)
VSWR	2.0 to 1	3.0 to 1 Maximum 2.0 to 1 Typical
Power	60 W average	60 W average
Pattern	Omnidirectional	Omnidirectional
Switching Time	100 Microseconds	1 to 3 Milliseconds (3)
Height	Low	27 inches
Weight	Light	6 pounds

Notes: 1. At pattern peak
2. At horizon
3. 100-microsecond switching time can be achieved with a simple modification to the switching circuits.

5.3 ACKNOWLEDGEMENTS

The development of this antenna was accomplished with the assistance of many people, both at Hazeltine and at AVRADA. The authors acknowledge the contributions of J. Brune, F. Cansler, and O. Schoenberger at AVRADA for their advice and assistance with the measurements on the OH-58A; and the technical consultation of Dr. H. A. Wheeler of Hazeltine.

SECTION VI

REFERENCES

1. Medgyesi-Mitschand, L. N. and Putnam, J. M. "Prediction of VHF/FM Antenna Radiation Patterns," ECOM-77-3036-F Final Report, September 1977.

2. Wheeler, H. A. "Fundamental Limitations of Small Antennas," Proc. IRE, Vol. 35, No. 12, December 1947, pp. 1479-1488.

3. Fano, R. M. "Theoretical Limitations on the Broadband Matching of Arbitrary Impedances," Res. Lab. Electronics, MIT Tech Report 41, January 1948.